HAL

archives-ouvertes.fr

Fate of cadmium in the rhizosphere of Arabidopsis halleri grown in a contaminated dredged sediment

Stéphanie Huguet, Marie-Pierre Isaure, Valérie Bert, Agnès Laboudigue, Olivier Proux, Delphine Vantelon, Anne-Marie Flank, Géraldine Sarret

▶ To cite this version:

HAL Id: hal-01256222

https://hal-mines-paristech.archives-ouvertes.fr/hal-01256222

Submitted on 18 Jan 2016

Fate of cadmium in the rhizosphere of *Arabidopsis halleri* grown in a contaminated dredged sediment.

Huguet Séphanie[a,b,c,d], Isaure Marie-Pierre[b], Bert Valérie[c], Laboudigue Agnès[d,1],

Proux Olivier[e], Flank Anne-Marie[f,g], Vantelon Delphine[f,g] and Sarret Géraldine[a]

[a] ISTerre, Université Grenoble Alpes, CNRS, F-38041 Grenoble, France.

[b] Laboratoire de Chimie Analytique Bio-Inorganique et Environnement (LCABIE), Institut des sciences analytiques et de physico-chimie pour l'environnement et les matériaux (IPREM UMR 5254), Université de Pau et des Pays de l'Adour and CNRS, Hélioparc, 2 Av. Pierre Angot, 64053 Pau Cedex 9, France.

[c] INERIS, Parc technologique Alata, 60550 Verneuil-en-Halatte, France.

[d] EMDouai, MPE-GCE, 930 Boulevard Lahure, 59500 Douai, France.

[e] OSUG, UMS832 CNRS/UJF, 414 rue de la piscine, 38400 Saint –Martin d'Hères, France.

[f] Beamline LUCIA, SLS, Swiss Light Source, CH-5232 Villigen, Switzerland.

[g] Synchrotron SOLEIL, F-91192 Gif Sur Yvette, France.

[1] Present address: Ecole des Mines de Paris, 60 boulevard St Michel 75272 Paris Cedex 06, France

Corresponding authors:

huguet.st@gmail.com

geraldine.sarret@ujf-grenoble.fr

Abstract

In regions impacted by mining and smelting activities, dredged sediments are often contaminated with metals. Phytotechnologies could be used for their management, but more knowledge on the speciation of metals in the sediment and on their fate after colonization by plant roots is needed. This work was focused on a Zn, Cd-contaminated contaminated dredged sediment from the Scarpe river (North of France). Zn, Cd hyperaccumulating plants *Arabidopsis halleri* from metallicolous and non metallicolous origin were grown on the sediment for five months in a pot experiment. The nature and extent of the modifications in Cd speciation with or without plant were determined by electron microscopy, micro X-ray fluorescence and bulk and micro X-ray absorption spectroscopy. In addition, changes in Cd exchangeable and bioavailable pools were evaluated, and Cd content in leachates was measured. Finally, Cd plant uptake and plant growth parameters were monitored. In the original sediment, Cd was present as a mixed Zn, Cd, Fe sulfide. After five months, although pots still contained reduced sulfur, Cd-bearing sulfides were totally oxidized in vegetated pots, whereas a minor fraction (8%) was still present in non vegetated ones. Secondary species included Cd bound to O-containing groups of organic matter and Cd phosphates. Cd exchangeability and bioavailability were relatively low and did not increase during changes in Cd speciation, suggesting that Cd released by sulfide oxidation was readily taken up with strong interactions with organic matter and phosphate ligands. Thus, the composition of the sediment, the oxic conditions and the rhizospheric activity (regardless of the plant origin) created favourable conditions for Cd stabilization. However, it should be kept in mind that returning to anoxic conditions may change Cd speciation, so the species formed cannot be considered as stable on the long term.

1. Introduction

The North of France hosts one of the oldest and largest industrial areas in Europe, with a large concentration of non-ferrous metal processing activities. The Scarpe river is strongly

impacted by these activities, and sediments are contaminated by many metals including Zn (about 7000 mg kg^{-1}) (Isaure et al., 2002) and Cd (about 600 mg kg^{-1}) (Alary and Demougeot-Renard, 2008). The maintenance of waterways such as the Scarpe river by regular dredging generates large volumes of metal-polluted sediments. Land disposal of these sediments may present some risks in the environment. Sediments with contaminant levels above guidelines are usually stored in landfill sites. Over the last decade, a substantial body of research has been conducted on the fate of metals in the lower Scarpe river. Studies have focussed on the speciation of Zn (Isaure et al., 2002; Isaure et al., 2005) and other metals (Thiry *et al.*, 2002) and on their availability (Piou et al., 2009; Lions et al., 2010). Chemical extractions suggested that Cd was mostly present in the oxidable fraction, likely polymetallic sulfides, but no direct methods such as EXAFS spectroscopy was used to determine Cd overall speciation in this sediment. Chemical extractions suggested that after land disposal of the sediment, the sulfidic pool progressively decreased in favour of exchangeable forms (Piou et al., 2009). Secondary Cd species formed after release of Cd^{2+} in a soil may include O-coordinated Cd adsorbed to iron oxihydroxides, clay minerals, carbonates and COOH/OH groups of organic matter, and S-coordinated Cd complexed by reduced organic S groups of natural organic matter or bacterial cell walls or Cd adsorbed to metal sulfides (O'Day et al., 1998; Karlsson et al., 2005, 2007; Sajidu et al., 2008; Mishra et al., 2010; Fulda et al., 2013). To our knowledge, there is no study on Cd speciation in dredged sediments after land disposal using direct methods.

Phytotechnologies have been proposed as alternative management methods for these sediments (Bert et al. 2009; Bolan et al., 2011). In a previous work, the fate of Zn after a phytostabilization treatment with graminaceous plants was studied (Panfili et al, 2005). Results showed a clear impact of the rhizospheric activity on Zn speciation, regardless of the plant species (*Festuca rubra* or *Agrostis tenuis*) and of the addition of amendments. Zn sulfide, present as major Zn species in the original sediment, was almost completely oxidized and replaced by secondary forms including Zn phosphate, Zn phyllosilicates and Zn-sorbed ferrihydrite. The rhizosphere is a zone of intense and dynamic exchanges between the soil, the root, and the microbial and fungal communities which colonize this zone. Exchanges in gas, water, solutes, large and small organic molecules are supposed to influence the chemistry of metals, although it is difficult to know exactly the role of each parameter in this complex interplay (Hinsinger et al., 2006; Wenzel 2009). The rhizosphere of metal hyperaccumulating plants has been the subject of many studies. Enhanced metal uptake by these species does not seem to be related to specific phenomena, but to the enhancement of processes common with non-accumulators. They include a highly developed root system, enhanced transport activity

at the soil-root interface, and possibly enhanced release (or release of different types) of organic ligands (Wenzel, 2003; Li et al., 2013, Tsednee et al., 2014). *A. halleri* is a model of Zn, Cd hyperaccumulating plant, and it has been intensively studied for the genetics and physiology of metal tolerance and hyperaccumulation (Roosens et al., 2008; Sarret et al., 2009; Huguet et al., 2012; Verbruggen et al, 2013; Isaure et al., 2015; Meyer et al., 2015). It is a pseudo-metallophyte, which means that it is found both on metal-rich and normal environments. Previous studies suggested some variations in metal tolerance and accumulation between and within populations (Meyer et al., 2010; Meyer et al. 2015). Despite these numerous studies, data concerning the impact of *A. halleri* on the speciation and availability of Cd in the soil are lacking.

The aim of this work was to determine the speciation of Cd in a dredged sediment, to assess its fate after land disposal, and to evaluate the influence of the rhizospheric activity on Cd speciation. The Cd tolerant and hyperaccumulating species *A. halleri* was chosen as model plant for this study because this species is naturally present in metal-contaminated soils of this studied area. Moreover, we have some knowledge on Zn and Cd tolerance and accumulation (Sarret et al., 2009 and Isaure et al., 2015, respectively), and on rhizospheric processes (Barillot et al., 2013) for *A. halleri* from the same metallicolous origin. Thus, this species was not chosen as a candidate for phytoextraction (which it is not), but as a model plant to study rhizospheric processes.

Information on Cd solid phase speciation, on Cd extractability and leachate composition, and on Cd transfer in the plant was obtained. Such combined approach provides key information on metal dynamics in soil–plant system both on the short and long term. Such knowledge is essential for the management and phytomanagement of dredged sediments after land disposal. In this aim, a 5-month pot experiment was conducted on a Zn- and Cd-contaminated dredged sediment with *A. halleri* of two origins, metallicolous (MET) and non-metallicolous (N-MET). Plants originating from a contaminated site and a non contaminated site were compared to examine potential differences between MET and N-MET plants in Cd uptake and Cd behaviour in rhizosphere. The speciation of cadmium in the sediment before and after culture and its relationships with other elements were studied by a combination of bulk and microanalyses including scanning electron microscopy coupled with energy dispersive spectroscopy (SEM-EDS), micro X-ray fluorescence (μXRF) coupled with Cd L_{III}-edge and S K-edge micro X-ray absorption near edge structure (μXANES) spectroscopy, and bulk Cd K-edge extended X-ray absorption fine structure (EXAFS) spectroscopy. The mobility and bioavailability of cadmium in the sediment were studied by $Ca(NO_3)_2$ extractions and

diffusive gradient in thin films (DGT), and measurement of Cd content in the leachates. In addition, plant growth parameters and Cd accumulation were monitored.

2. Materials and methods

2.1 Sediment

The sediment was collected from the lower Scarpe river in the North of France (about 30 km south of Lille). In this study, 500 kg of surface sediment from an area containing 150 mg kg^{-1} Cd (Alary, 2001) were dredged with a mechanic shovel. The sediment was then mixed, spread as a 20 cm-thick layer and dried outdoor for 7 months until the water content was 20 % in mass. The sediment was mechanically homogenized several times and sieved (< 5 mm with a Cross Beater Mill SK – RETSCH). Characteristics of the sediment at this time, "initial time" *ti* (Fig. 1), just before plant culture, are given in Table 1. Particle size distribution was analyzed following methods described in Isaure et al. (2002). Pseudo-total elements concentrations (Cd, Zn, Cu, Pb, Ni, and As) were quantified in sediment and in the different granulometric fractions. Aliquots of 0,5 g of samples were dried and sieved (100μm) and then digested by aqua regia micro-waves assisted dissolution. Metal concentrations were determined by ICP-AES. Quality control was based on the use of sediment certified standard samples (NWRI TH-2) and internal control samples.

The pH of the sediment before culture was about 7.48 ± 0.01. The sediment was relatively rich in organic matter and had a relatively high cation exchange capacity (Table 1). As expected the metal concentrations in sediment were high with 141 ± 24 mg kg^{-1} Cd, and other metals (Table 1). The Cd content was higher in finest fractions (e.g. 290 ± 10 mg kg^{-1} Cd for <2μm fraction). Sediment was mainly composed by <50 μm fractions (Table 1), which concentrated 72 % Cd.

2.2 Plant material

A. halleri develops natural populations on both metal contaminated and uncontaminated soils in Europe (Bert et al., 2002). Viable seeds of *A. halleri* were collected in a smelter-impacted site (Bois des Asturies - Auby, France) and in an uncontaminated site (Hautes Fagnes, Belgium). The soil of Bois des Asturies has been characterized in several studies (Bert et al., 2000; Cuny et al., 2004; Sarret et al., 2004; Pauwels et al., 2006; Farinati et al., 2011; Gomez-

Balderas et al. 2014). The data from Sarret et al. (2004) are given in Figure SI-1. The topsoil (0-20 cm) in which *A. halleri* developped roots was collected, and characterized as previously described for the sediment (Fig. SI-1).

2.3 Pot experiment

After vernalisation, *A. halleri* seeds were germinated on filter papers moistened with deionized water. Seedlings were transferred to pots filled with compost and grown for 4 weeks. Just before transfer on sediment (at *ti* – Fig. 1), metals concentrations in aerial parts of *A. halleri* seedlings of both origins were analysed. Seedlings of *A. halleri* from metallicolous (MET) and non metallicolous (N-MET) origin were transferred to 4 L pots containing 2,8 kg of 5 mm-sieved sediment after roots had been washed carefully with deionised water. The monitoring of the culture was started after a 3-weeks period of adaptation to the new substrate (at t_0). Non vegetated pots were used as control, and each vegetated pot contained one seedling. A total of 39 pots were used, including 3 for the control and 18 for each origin of *A. halleri* (a triplicate for each sampling time, t_0 to t_5). Sediment moisture was maintained at 80% field water capacity by regular addition of deionised water. Plants were grown for five months in controlled conditions (12h photo period, 20/16°C day/night temperature, 80 % relative humidity) and pots were moved randomly each week.

2.4 Microscopic and spectroscopic analyses of the sediment before and after culture

Cd localization in the sediment was studied by SEM-EDS and µXRF. Cd speciation was studied by Cd K-edge bulk EXAFS spectroscopy and Cd L_{III}-edge µXANES spectroscopy, and S speciation was determined by S K-edge µXANES spectroscopy.

2.4.1 Sample preparation

Undisturbed blocks of sediments were collected from the pots before and after culture with MET and N-MET plants. Rhizosphere blocks were then freeze-dried, impregnated with epoxy resin, and prepared as 30 µm-thick micro-polished thin sections for electron and X-ray analyses (SEM-EDS, µXRF and µXANES). For bulk analyses, other blocks from pots with or without plant were collected. Roots were removed, and the substrate was freeze-dried, ground and pressed as pellets.

2.4.2 Reference compounds

The XANES and EXAFS analysis was based on a large database of reference Cd-containing compounds. They included commercial Cd minerals, Cd-containing compounds prepared at the laboratory and natural samples. Purchased chemicals used were all ACS reagent or analytical grade quality. The database included CdS, $CdCl_2$, $CdCO_3$, $Cd(NO_3)_2$, CdO, $Cd(OH)_2$, Cd-phosphate ($Cd_5H_2(PO_4)_4$, $4H_2O$), $CdSO_4$, Cd-sorbed goethite and Cd-sorbed ferrihydrite containing ~8000 mg kg^{-1} Cd kindly provided by A. Voegelin (Fulda et al., 2013), and a mixed sulfide (Zn, Cd, Fe)S extracted from a metamorphic rock was used as well. It was composed of sphalerite enriched in Cd and Fe (XRD spectrum in Figure SI-2 – Cd content: 1350 ppm). In addition, a library of Cd-organic complexes including Cd-malate, Cd-citrate, Cd-succinate, Cd-alginate, Cd-histidine, Cd-cysteine, Cd-glutathione, Cd-PC2, Cd-oxalate, Cd-cellulose, Cd-pectin, already described by Isaure et al. (2006, 2015) and Huguet et al. (2012) was used. Two more reference compounds included Cd with three organic acids in solution (Cd-OAs, 5mM Cd, 14mM citrate, 100mM malate and 400 mM succinate at pH=5.5 - concentrations were chosen according to PHREEQC calculation to have equivalent concentrations of $(Cdsuc_2)^{2-}$, Cdsuc, $(Cdcit_2)^{4-}$, $(Cdcit)^-$, Cd^{2+}, Cdmal complexes); and free Cd^{2+} (10mM Cd^{2+} at pH = 2.2). Solid state references were diluted in boron nitride and pressed as 5 mm diameter pellets. All solutions reference compounds were mixed with 20% glycerol to prevent ice crystal formation during cooling. Spectra for all Cd-containing references were recorded at Cd K-edge and L_{III}-edge. For S K-edge XANES analyses, the database presented in Sarret et al. (1999) was used.

2.4.3 Data acquisition

Micro-analyses were performed on thin sections of sediment samples. Cd-rich regions and geochemical associations were first investigated by environmental SEM-EDS. For the sediment before culture, we used a Quanta 200, FEI interfaced with a RONTEC single Drift detector. The chamber pressure was 0.45 Torr and the accelerating voltage 20 kV. Ten Cd-rich regions areas were identified. For the sediment after culture, we used a Hitachi S-4300 environmental scanning electron microscope with Thermo Ultradry Silicon Drift detector, using an acceleration voltage of 20 kV and pressure was 3990 Torr (30 Pa). Twelve Cd-rich regions areas were analyzed (6 for sediment with MET plants and 6 for sediment with N-MET plants). μXRF and μXANES analyses were performed on beamline LUCIA (SLS, Villigen, Switzerland) equipped with Si (111) crystals and a SDD fluorescence detector, with a beam size of 2.5 x 5 μm on the sample and at room temperature. Regions of interest

identified by SEM were mapped by µXRF before recording Cd L$_{III}$-edge (3538 eV) and S K-edge (2472 eV) µXANES spectra. For each sample, 6 to 8 XANES scans of 20 min were averaged. Cd L$_{III}$-edge and S K-edge XANES spectra were also recorded in unfocused mode on various Cd- and S-containing references (see above). For reference compounds, 2 to 3 spectra were averaged.

Cd K-edge bulk EXAFS measurements were performed on sediment samples on the beamline FAME (BM30B – Proux et al., 2006) at the European Synchrotron Radiation Facility (ESRF, Grenoble, France) equipped with a Si (220) double crystal monochromator. Pellets of sediment samples and reference compounds (pellets and solutions) were transferred in a liquid He cryostat cooled to 15 K. Spectra were recorded in fluorescence mode using a 30-element solid-state Ge detector (Canberra). For each sample, 10 to 17 scans of 40 min were averaged.

2.4.4 µXRF and XAS data treatment

For µXRF elementary maps, fluorescence intensities were normalized by the incident photon intensity (I0) and counting time. XAS spectra were treated using ATHENA (Ravel, 2009) software. The calibration of energy was done using a metal foil reference by setting the first inflexion position of Cd-metal XANES spectrum to the tabulated value of 26711 eV; the contribution of the matrix was subtracted and a normalization of signal was done using a linear or a two-degree polynomial. The extracted EXAFS was then k^3-weighted to enhance the high-k region, and Fourier-transformed (FT) over the k range 3.0 to 10.5–13 Å^{-1}, depending on the level of noise. The proportions of Cd species in sediment samples were obtained by least-squares fitting of recorded spectra to linear combinations of reference spectra from a library of Cd model compounds including Cd-substituted and Cd-sorbed minerals and Cd-complexed organic compounds (see above). For each spectrum, LCFs using one, two and three components were tested successively. The fit with $n+1$ components was retained if the normalized sum-squares residual ($NSS = \sum[k^3\ \chi_{exp} - k^3\ \chi_{fit}]^2 / \sum[k^3\ \chi_{exp}]^2\ 100$) was decreased by more than 10 % as compared to the fit with n components. Percentages of Cd species are given as average and standard deviations presented are the average over satisfactory fits, defined by NSS comprised between the value obtained for the best fit (NSS_{best}) and 1.1 NSS_{best}.

In parallel, from k^3 EXAFS spectra, the structural parameters for Cd reference compounds and sediment samples were determined by shell simulations using ARTEMIS (Ravel & Newville, 2005). Phase and amplitude functions were calculated by FEFF 6.0 using the structure of greenockite (CdS) and cernyite (Cu$_2$(Cd$_{0.37}$Zn$_{0.33}$Fe$_{0.29}$)SnS$_4$) (Szymanski, 1978), Cd-organic

structures from the Cambridge Structural Database (CSD, Bruno et al., 2002) and the structure of $Cd_5H_2(PO_4)_4$, $4H_2O$. EXAFS spectra were Fourier transformed over a k range of 3.2–11 Å for sediment samples, and the contribution of the first shell was simulated in R space, either with O atoms only, or with O and S atoms.

S K-edge XANES spectra were treated by LCFs as described above. S reference compounds were grouped into three families: mineral sulfides (including CdS and (Zn, Cd, Fe)S), organic sulfides (including R-SH, R-S-R and R-S-S-R groups) and oxidized sulfur (including sulfoxides, sulfone, sulfonic acid, and sulfates).

2.5 Monitoring of Cd in sediment, plant and leachates

A monthly monitoring of the sediment, plants and leachates was performed for five months. Each month, three pots per condition were removed from the experiment for the analysis of the sediment and plant. The sediment was separated manually from the roots, sieved (< 2 mm), and total metals concentrations, pH, total carbon (TC) and metals exchangeable and phytoavailable pools were measured on triplicates.

The $Ca(NO_3)_2$ exchangeable pool was measured according to (Bert et al. 2012). After sieving (< 2 mm) and drying the sediment at 60°C, 10 g (DW) were shaken in 20 mL $Ca(NO_3)_2$ 0.01 N (analytical quality in ultrapure water) for 48 hours at room temperature. After centrifugation (20 min at 1200 g), filtration (0.45 μm), and acidification of the supernatant (0.5 mL of concentrated, supra-pure nitric acid), metal concentrations were determined by ICP-AES.

Metals phytoavailability was estimated by diffusive gradient in thin film (DGT) probes (Zhang *et al.*, 2001, Nolan *et al.*, 2005). DGT devices loaded with a 0.4 mm resin gel layer (chelex gel), a 0.7 mm diffusive gel layer (polyacrylamide gel, restrictive pore) and a 0.13 mm filter (cellulose nitrate) were provided by DGT Research Ltd. 100 g of sieved sediment were wet to 100 % field water capacity, manually mixed to make a smooth paste, and finally shaken for 3 days. DGT were pressed gently onto the surface of the sediment and placed for 17h between 20°C and 24°C. Metal analyses and determination of C_{DGT} were made by ICP-MS or AAS by DGT Research Ltd.

Plant aspects were examined and rosette diameters were measured on a monthly basis. Besides, on monthly removed pots, three plants of each origin were harvested to analyze their

aboveground parts (biomass and metals concentrations). Aerial parts were washed with deionised water, oven-dried at 40°C until constant weight, then biomass was weighed, ground and homogenized to prepare one aliquot per pot. Total concentrations of Cd in plant tissues were determined after digestion of 1 g dry matter in 10 ml of HNO_3 and 3 ml of H_2O_2, in a microwave oven. Solutions were filtered, adjusted to 100 ml with Milli-Q® water and stored at 4°C before analysis. Cd concentrations in the digests were determined by ICP-AES. Spinach leaves samples (SRM 1570a) were used as certified standard.

The monitoring of leachates was performed monthly on the same three pots (cultivated or not). Leachates were collected at the bottom of the pots after the substrate (cultivated and non-cultivated) had been watered with 1 L of deionised water, delivered in small volumes (200 mL). Leachates were collected for 2 hours after watering. Leachates were filtered (0.45 µm), then aliquots of 10 mL were acidified with HNO_3 (suprapur®) and stored at 4°C before analysis. Metals concentrations were determined by ICP-AES for which quality control was based on the use of internal control samples.

Statistic analysis was performed using two and one-way ANOVA followed by post hoc comparison using Tukey's test for comparison of individual means (statistical program SPSS 15.0 (2007)).

3. Results

3.1 Cd speciation in the sediment before and after culture of *A. halleri*

3.1.1 Average Cd speciation by Cd K-edge bulk EXAFS spectroscopy

The speciation of Cd in the sediment before and after culture was examined by EXAFS spectroscopy. Representative Cd K-edge EXAFS reference spectra used for the linear combination fits are shown in Figure 2. Figure 3 shows the sediment spectra and LCFs results. The spectrum for the sediment before culture was correctly reconstructed with 100% (Zn, Cd, Fe)S (Fig. 3). Adding a second component did not improve significantly the fit (not shown). Thus, Cd was mainly present as a mixed metallic sulfide. Spectra for the sediment after culture with *A. halleri* MET and N-MET, and for the control (*i.e.* non vegetated) sediment were similar, although the later presented slightly lower amplitude oscillations, in particular at 11 Å^{-1} (Fig. 3A). Cd in the non vegetated pot was present as 74 ± 2 % Cd-

Organic acids, 22 ± 1 % Cd-phosphate and 8 ± 1 % Cd as mixed sulfide ((Zn, Cd, Fe)S - Fig. 3B). Removing this later species increased the fit residual by 11 %. Thus, although the proportion of Cd mixed sulfide is within the precision of the method as generally estimated (± 10 %), its contribution may be significant in the present case. At the opposite, spectra for vegetated sediment were correctly fitted with a combination of Cd-organic acids 64 ± 5 % and 61 ± 16 % for MET and N-MET respectively) and Cd-phosphate (34 ± 2 % and 30 ± 16 % respectively). These results evidence changes in Cd speciation during the pot experiment. Cd sulfide was almost completely oxidized in the absence of plants, and secondary phases including Cd-organic complexes and Cd phosphate were formed. The same process was observed in the presence of plants, but the removal of Cd sulfide was total and the proportion of Cd-phosphate increased. There was no influence of the origin (MET or N-MET) of *A. halleri* on Cd speciation in the substrate.

Structural parameters for Cd in the sediment and several representative Cd reference compounds were then determined by shell fitting (Fig. 4, Table 2). For CdS, Cd-phosphate and $CdCO_3$, structural parameters were consistent with the XRD structures (Huguet et al., 2012). For (Zn, Cd, Fe)S, the first shell of coordination was simulated by 4 S atoms at 2.52 Å, as in CdS structure, and the second shell by a mixture of Fe, Zn and Cd atoms (Table 2, Fig. SI-3). As expected, the same type of environment was obtained for the sediment before culture. Fit with Cd only as next nearest neighbour was not satisfactory (Fig. 4B). Based on the Fe, Zn, Cd coordination numbers (0.3, 4.8 and 2.2, respectively, Table 2), it can be concluded that Cd was present as a mixed sulfide containing about 2/3 Zn, 1/3 Cd and traces of Fe. The sum of Zn, Cd and Fe contributions was 7.3 atoms, *i.e.* significantly lower than the 10 atoms in CdS or ZnS structure, but like in the (Fe Zn Cd)S reference, *i.e.* about 8 neighbours in the second shell. This difference likely reflects some structural disorder, probably due to the presence of metals with very different ionic radii in the crystal lattice, and/or to the presence of non-equivalent crystallographic sites for Cd. The Fourier transformed spectra for the sediments after the pot experiment showed a first shell at a distance typical of oxygen ligands, and almost no second shell peak (Fig. 4B). For the vegetated pots, fit results gave 6-7 O atoms at 2.29-2.3 Å (Table 2). For the non vegetated pot, a minor contribution of S atoms was found, which is consistent with LCFs results. Due to the very low amplitude, no significant signal was observed for R+ΔR > 2.5 Å: no second shell was needed for the simulation.

3.1.2   SEM-EDS, micro-XRF and Cd-L_{III} edge and S-K edge μXANES analyses

Micro-scale investigations were performed to observe geochemical associations, weathering processes of Cd sulfide grains, and to identify possible minor forms of Cd in sediment before and after culture. SEM-EDS enabled the localization of Cd-rich regions in various types of grains. A representative coarse grain of the sediment before culture is shown in Figure 5, and two representative grains for the sediment after culture are shown in Figure 6. For the sediment before culture, metal-rich areas were localized at the edge of the grain (Fig. 5A, B). The Cd richest region contained Zn and S as major elements (40 and 31 % in atomic % based on the EDS calculated composition), as well as Si (12 %), Al (6.9 %), Mg (3.1 %), Cd, Ca and Na (1.8 %), Fe (1.1 %). These results suggest the presence of Zn sulfide containing impurities of Cd and Fe, associated with aluminosilicates nanoparticles. These findings are consistent with bulk EXAFS results. Other regions contained more diffuse Cd concentrations around Cd-rich spots. Two spots were selected for µXANES analyses, the Cd rich spot described above (P2, with S/Cd fluorescence intensity ratio = 8 and P/Cd = 0.4, Fig. 5B), and a spot with more diffuse Cd concentration (P1, with S/Cd = 21 and P/Cd = 0.8, Fig. 5B). Cd L_{III}-edge µXANES spectra recorded on the bulk sediment, on P2 and P1 are shown in Figure 7. They show a smooth edge characteristic of S ligands (Isaure et al., 2006). They were all fitted with 100 % Cd sulfide species. (Zn, Cd, Fe)S was the only component for the bulk sediment and the Cd richest spot (P2), whereas Cd-thiols (Cd-organic sulfides) were present as additional component in P1 (Fig. 9). Figure 7 shows that the spectrum for Cd-thiol has some similarities with CdS and (Zn, Cd, Fe)S, but is smoother.

In addition, S K-edge µXANES were recorded in the bulk sediment and on P1 and P2 spots to investigate S oxidation state (Fig. 8). They all showed a first peak at 2473 eV, characteristic of reduced S (Fig. 8). In addition, P1 shows a peak at 2482 eV (Fig. 8) characteristic of oxidized S. Three families were distinguished by LCFs, including mineral sulfides, organic sulfides and oxidized S species. Mineral sulfides dominated in the bulk and in P1 and P2 spots, organic sulfides represented minor species in P1 and P2 spots, and oxidized species represented 4 % (in the bulk) to 12 % (in P1 - Fig. 9).

Two representative grains for the sediment after culture showed reddish brown area around the grains that indicated the presence of oxidized Fe (Fig. 6A). SEM-EDS analyses showed that Cd-rich region contained also S, Fe, Zn, Si, Al and P in various proportions (Fig. 6B). Micro-XRF maps allowed to localize the Cd most concentrated spot previously identified by SEM and to visualize more precisely the chemical associations. The Cd richest spot, P3A, contained also S and P (Fig. 6B). Another Cd-rich spot, P3B, was less rich in S and P than

P3A (Fig. 6B). The spot P3C contained less Cd (Fig. 6B). The second representative grain shows a zone with diffuse Cd co-localized with P, and to a lesser extent with S (spot P4, Fig. 6C). The Cd L_{III} μXANES spectra for P3A and P3B were similar to P1 and P2, whereas P3C and P4 spectra presented a pre-peak at 3538 eV characteristic of Cd-O bond (Fig. 7). Based on LCFs, the Cd richest spots (P3A and P3B) contained a majority of Cd sulfides and 15 to 25 % Cd Cd-organic acids, whereas the more diffuse zones (P3C and P4) contained Cd-organic acids and Cd-phosphate as major species (80 and 100 %, respectively – Fig. 9). Thus, Cd speciation drastically changes from P3B to P3C which are distant of about 50 μm. The presence of Cd phosphate is consistent with the high P signal in spot P4. The chemical state of S as determined by S K-edge XANES showed an increase in oxidized S species following the increase in Cd-O species. The spot containing the higher amount of oxidized S is P4, with 34 % (Fig. 9). In this spot, Cd-S species were completely replaced by Cd-O species. Thus, other sulfide species, more resistant to oxidation than the one hosting Cd, are still present. Again, spots distant of 50 μm only showed very different S speciation. These results were obtained on the sediment vegetated with MET plants. Very similar results were obtained with N-MET plants, therefore these results are not presented here.

To conclude, the persistence of Cd sulfide species in some Cd rich spots was observed in the sediment after culture. These species represent less than 10 % of total Cd since they were not detected by bulk XAS. In addition, a large variety of S oxidation states was observed, but reduced S dominated, even in spots where Cd sulfides species had been oxidized.

3.2 Cd exchangeability and leaching

XAS is not very sensitive to weakly sorbed species, and it is useful to evaluate in parallel the exchangeable and bioavailable pool at the macroscopic scale by physico-chemical approaches. Cd pseudo-total concentration in sediment before culture was about 140 mg kg^{-1} (Tab.1) and was not significantly different than those measured in sediment during and after culture with MET or N-MET plants and in control pots, *i.e.* without plant (not shown). However, after culture, a decrease of approximately 0.6 pH unit was observed in pots with plants (regardless their origin) and in control pots (ANOVA 1 factor P>0.05 - not shown). Indeed the pH measured before culture in sediment at 7.48 ± 0.01 (Tab.1) was then measured at 6.86 ± 0.22, 6.95 ± 0.03 and 6.81 ± 0.02 for MET, N-MET and control pot respectively. Decrease in pH measurement was not a plant effect. It was probably correlated with oxidation of metallic sulfides in sediment.

For the sediment before culture, $Ca(NO_3)_2$-extractable Cd concentration was 1.02 ± 0.1 mg kg^{-1} DW (Fig. 10A). At the end of the monitoring, this parameter decreased significantly in the control pot (P<0.05, 0.71 ± 0.03 mg kg^{-1} DW at t_6 for control pot, Fig. 10A). For vegetated pots, extractable Cd concentrations measured monthly were significantly different from the sediment before culture, even after only one month (P<0.05, Fig. 10A). However, they were not significantly different from those measured in the control pot at t_6 (P>0.05, Fig. 10A). Thus, there was no plant effect on Cd extractable concentrations during culture regardless of *A. halleri* origin.

DGT was used to quantify Cd phytoavailable pool in sediment for some samples (Fig. 10B). Cd bioavailable concentrations were lower than Cd extractable concentrations. By comparison with Cd extractable concentrations, there was no significant difference between bioavailable Cd in the sediment before culture and in vegetated pots (Fig. 10B). Bioavailable Cd was not measured on pots without plant at the end of the assay.

Thus, the major changes in Cd speciation observed between the sediment before and after culture did not induce marked changes in Cd exchangeability and bioavailability.

The evolution of Cd concentrations in leachates was monitored monthly (Fig. 11A). For control pots, Cd concentrations were not significantly different over time (P>0.05 – Fig. 11A): about 0.30 ± 0.07 mg L^{-1}. By contrast, in vegetated pots Cd concentrations were lower from t_2 and then did not vary significantly (Fig. 11A). Thus, the presence of plants seems to decrease Cd concentrations in leachates.

3.3 Cd transfer in the plant

The plant biomass was measured monthly. At *ti*, when plants were transferred on sediment, plants of both origins presented similar biomasses, *i.e.* 3.0 ± 1.1 g for MET plants and 3.2 ± 1.7 g for N-MET (average for n=3 $\pm$ SD, (P>0.05, test of Student - Fig.11B). Biomasses measured after one month of growth, i.e. at t_1, were higher than those measured at *ti* (Fig. 11B). This shows that plants were able to develop on contaminated sediment. No significant increase of biomass was observed for N-MET plants between t_1 and t_5 (P>0.05, Fig. 11B), but standard deviations were important. MET plants biomass increased from t_1 to t_3 and then decreased (P<0.05, Fig. 11B). The maximum difference in biomass was observed the third month (33.1 ± 4.6 g for MET), and could be related to a better tolerance of metallicollous

plants compared to non metallicolous ones (Meyer et al. 2015) as shown for Zn (Meyer et al., 2010). During the fourth month of culture, one part of MET plant leaves began to show drought signs. The decrease in biomass observed at t_4 and t_5 could be a response to sediment toxicity.

Cd concentrations were measured in aerial parts of *A. halleri* at *ti* as follow: 3.7 ± 2.4 and 4.7 ± 1.0 mg kg^{-1} DW for MET and N-MET plants respectively (Fig. 11C). There was no significant difference between plant origins (Student test: P>0.05). From t_1 to the end of growth, Cd concentrations were higher than those measured at *ti*. For instance, between *ti* and t_1 Cd concentrations in aerial parts were respectively increased by 30 and 39 times for MET and N-MET. All measured concentrations, except for N-Met at t_2, reached the hyperaccumulating threshold set to 100 mg Cd kg^{-1} DW (Baker and Brooks, 1989, Wenzel and Jockwer, 1999). For each origin tested separately, no significant variation of Cd concentrations in aerial parts was observed with time (P>0.05, Fig. 11C). Maximal Cd concentrations were 204 ± 96 and 185 ± 18 mg kg^{-1} (n=3 $\pm$ SD) for, respectively, MET plant at t_4 and N-MET plant at t_1 (Fig. 11C). Standard deviations were important, suggesting a high inter-individual variability in Cd accumulation.

4. Discussion

4.1 Cd speciation in sediment before and after culture of *A. halleri*

Before culture, Cd in the sediment was present as a mixed Cd,Zn,Fe-sulfide containing about 2/3 Zn, 1/3 Cd and traces of Fe. Cd-containing mixed sulfides were also observed in metal-contaminated marine sediments (O'Day et al.; 1998; Carroll et al., 2002). A previous study on Zn speciation in the Scarpe sediment showed that Zn was mostly present as sphalerite (Isaure et al, 2002). Considering that Zn is 25 to 30 times more concentrated than Cd in this sediment (Table 1), it is clear that the sediment contains both some mixed Cd,Zn,Fe-sulfides and pure Zn sulfide. This was confirmed by SEM-EDS. Likewise, pure pyrite grains were observed by SEM-EDS (not shown), so Fe is present both in mixed metallic and pure Fe sulfide. Polymetallic sulfides may come from the ore which was transported by boat on the river, from atmospheric emissions of the smelters and dissemination of smelter slag (Isaure et al, 2002). They may also be formed during early diagenesis of sediments (Audry et al., 2005). The

presence of both reduced and oxidized forms of sulfur in the sediment shows that it has been partially oxidized during the drying and preparation procedure.

After 5 months of pot experiment, Cd sulfides were totally (for vegetated pots) and almost totally (8 % remaining Cd sulfides in non vegetated ones) oxidized, and secondary species included Cd-organic acids and Cd phosphates. Micro analyses confirmed the persistence of Cd sulfides in some regions of the sediment thin sections. The study of Zn speciation in dredged sediment from the Scarpe vegetated or not with two *Poaceae* (*Agrostis tenuis* and *Festuca rubra*) showed that after 18 months of culture, ZnS was almost completely oxidized, whereas half of Zn was still present as ZnS in the pot without plant (Panfili et al., 2005). Although plants and conditions differed between the two studies, the comparison of the results suggested a higher sensitivity to oxidation for Cd than for Zn in this sediment. Previous studies on mixed metallic sulfides suggested different sensitivities of metals towards oxidation, with preferential release of Zn relative to Cd (O'Day et al., 1998; Barret and McBride, 2007). The same tendency was observed in Zn, Cd-containing soils rich in sulfur (McBride et al., 2006; de Livera et al., 2011). These results are not in contradiction with our results because in the Scarpe sediment, Cd was mostly present in a mixed (Zn, Cd, Fe)sulfide, whereas Zn was mostly present as pure ZnS. Thus, the change in Zn speciation in this sediment is controlled by ZnS much more than by the mixed sulfide. The persistence of reduced S species in regions of the thin sections where Cd was bound to O ligands (see Results) suggests that other metallic sulfides are still present in regions where Cd has been oxidized.

In the sediment without plant, the oxidation of metallic sulfides may be ascribed to the alternating dry and wet conditions due to watering, which brings oxygen to the system. Barrett and McBride (2007) demonstrated that oxidation of inorganic sulfides to SO_4^{2-} in aerated soil environments proceeded within hours. In a study on Cd speciation in a paddy soil, Fulda et al. (2013) showed the formation of Cd sulfides under flooded (anoxic) conditions. The CdS crystallites, estimated to be nanometer-sized, were oxidized upon aeration of the system, and the original Cd speciation, dominated by Cd-carboxyl species, was restored. Like in acid mine drainage environments, the oxidation of metallic sulfides may be catalyzed by microorganisms. Bacteria present in sediments of the Scarpe River have been shown to play an important role in increasing or decreasing metal availability (Lors et al. 2004; Bert et al 2009, 2012). Bert al. (2012) suggested that bioleaching of metals was caused by sulfur-oxidizing bacteria whereas anaerobic sulfate-reducing bacteria could precipitate metals.

In the planted sediment, the oxidation process was slightly higher, although the difference is close to the uncertainty of the method. Several processes taking place in the rhizosphere might explain this oxidation: Plant rooting may increase the penetration of oxygen in the sediment. This effect counterbalances the effect of root respiration which, conversely, causes O_2-impoverishment and CO_2-enrichment of the rhizosphere (Marschner 1995; Hinsinger et al, 2003). The uptake of water, ions and nutrients and the release of ions and organic ligands by the root and associated organisms (fungi, bacteria) are supposed to affect the chemical equilibria and induce dissolution-reprecipitation and sorption-desorption processes.

In vegetated and non vegetated pots, Cd was mainly associated with phosphates (30-34 and 22 %, respectively) and with COOH/OH groups of organic matter (61-64 and 74 %, respectively). Cd phosphate can be considered as a stable species on the long term (Hamon et al., 1998). The role of organic matter in Cd binding in the Scarpe sediment after land disposal was highlighted by Vansimaeys et al. (2009), who evaluated by chemical extractions an increase from 10 to 65 % of organically bound Cd from the fresh to land deposited, drained sediment. Piou et al. (2009) also suggested an important role of organic matter in the control of the seasonal dynamics of Cd. The binding of Cd to COOH/OH groups of organic matter is consistent with previous findings by Liu et al. (2001) and Fulda et al (2013). Karlsson et al. (2007) identified a mixture of O- and S-containing ligands for Cd in a peat soil. The association of Cd with phosphate is not surprising because of the high P content of the sediment, and high affinity of Cd for phosphate minerals. The proportion of Cd phosphate was slightly higher in the vegetated than in the non vegetated pots. This can be related to the rhizosphere activity favouring the mobilization and increasing its availability (Hinsinger et al., 1998). The present EXAFS data do not allow to distinguish Cd-sorbed or coprecipitated phosphate, but both phenomena are likely (Brown et al. (2004).

4.2 Impact of *A. halleri* culture on Cd exchangeable pool and leachates

Although the presence of plants had an impact on Cd speciation in the sediment, they did not influence Cd exchangeable and phytoavailable pools. Both the Cd exchangeable and phytoavailable pools did not vary significantly with time for MET and N-MET plants. Low standard deviations indicated low variability between pots for these pools. The relative stability in the exchangeable and phytoavailable pools suggests that Cd sulfides on one hand, and the mixture of Cd phosphate and Cd-organic acids on the other hand, display similar exchangeabilities. This result suggest that the Cd-organic acid complexes are weakly

exchangeable. At the opposite, Zn-organic complexes found in Zn-contaminated organic soil were highly exchangeable (Sarret et al., 2004). The stability of Cd exchangeability during the experiment also suggests that Cd released by oxidation of sulfides was readily taken up by the secondary phases, with no transient phase with high Cd availability. The Cd content in the leachates was very low and the presence of the plant induced a decrease in Cd concentrations from the second month of culture. This phenomenon can be related to the colonization of the pot by roots and the development of a stable rhizosphere, decreasing the transfer of dissolved and particulate Cd. Plants grown on the sediment contained between 100 to 200 mg kg^{-1} Cd DW in their aerial parts. This relatively low Cd accumulation is consistent with the low Cd availability and with the fact that *A. halleri* is not a strong Cd hyperaccumulator (Huguet et al., 2012). The lack of difference in Cd solid state speciation, availability and leachability suggests that the rhizospheric activity of both plants have a similar impact on the soil chemistry. Additional data on root exudates, microbial activity and redox potential would be necessary to elaborate more on this point.

5. Conclusion

This study assessed the fate of Cd present in a contaminated dredged sediment during a pot experiment. The combination of chemical analyses and EXAFS spectroscopy allowed to elucidate chemical forms of Cd in the sediment before and after plant culture. Before culture, Cd was present as a mixed Zn, Cd, Fe sulfide. This mixed sulfide was relatively sensitive to oxidation since after 5 months of pot experiment, Cd-bearing sulfides were mostly oxidized in control pots without plants. The presence of *Arabidopsis halleri* seemed to enhance this process since Cd sulfides were totally oxidized in vegetated pots. Secondary species including Cd bound to O-containing groups of organic matter and Cd phosphates were formed both in vegetated and non vegetated pots. These changes probably occurred via both abiotic and biotic processes, and were enhanced by the plant activity. Despite these changes in speciation, there was no change in Cd exchangeability or phytoavailability. Cd phosphate can be considered as stable on the long term. Cd–organic matter complexes may not be stable on the long term, but their presence did not increase Cd phytoavailability during the experiment. This low availability and low transfer of Cd to leachates and plants are positive signals in terms of environmental management. A low Cd availability was also observed in the field after land application of the Scarpe sediment (Piou et al., 2009). The presence of plants is

supposed to give an added value to land disposal because of their role in the limitation of aerial dispersion of contaminants. This study shows that it also has a positive effect on Cd speciation. However, it is important to consider that Cd speciation may fluctuate depending on flooding and redox conditions (Piou et al., 2009; Fulda et al., 2013), and that Cd sulfide species may form again under flooded or saturated conditions. Thus, land application and vegetation of the sediment may be an interesting option, provided that the substrate remains unsaturated. .

Acknowledgements

References

Alary C. (2001) Technical report Douai - Fr., CNRSSP**:** 72.

Alary C. and Demougeot-Renard H. (2008) Fate of pollutant load in a small canalised river (Scarpe, North of France): understanding the spatial distribution of heavy metals in sediments using factorial kriging analysis. International Symposium on Sediment Management (I2SM), Lille, France.

Audry S., Blanc G. and Schäfer J. (2005) The impact of sulphide oxidation on dissolved metal (Cd, Zn, Cu, Cr, Co, Ni, U) inputs into the Lot-Garonne fluvial system (France). *Applied Geochemistry,* **20**, 919-931.

Baker A.J.M. and Brooks R.R. (1989). Terrestrial higher plants which hyperaccumulate metallic elements – a review of their distribution, ecology and phytochemistry. *Biorecovery* **1**, 81–126.

Barillot C.D.C., Sarde C.O., Bert V., Tarnaud E. and Cochet N. (2013). A standardized method for the sampling of rhizosphere and rhizoplan soil bacteria associated to a herbaceous root system. *Annals of Microbiology* **63** (2), 471-476

Barrett K.A. and McBride M.B. (2007) Dissolution of zinc-cadmium sulfide solid solutions in aerated aqueous suspension. *Soil Science Society of America Journal* **71**, 322-328.

Bert V., Macnair M.R., De Laguerie P., Saumitou-Laprade P. and Petit D. (2000) Zinc tolerance and accumulation in metallicolous populations of *Arabidopsis halleri* (Brassicaceae). *New Phytologist* **146**, 225–233.

Bert V., Bonnin I., Saumitou Laprade P., de Laguerie P. and Petit D. (2002) Do *Arabidopsis halleri* from nonmetallicolous populations accumulate zinc and cadmium more effectively than those from metallicolous populations? *New Phytologist*, **155**, 47-57.

Bert V., Seuntjens P., Dejonghe W., Lacherez S., Thuy H.T.T., Vandecasteele B. (2009) Phytoremediation as a management option for contaminated sediments in tidal marshes, flood

control areas and dredged sediment landfill sites. *Environmental Science and Pollution Research* **16**: 745-764.

Bert V., Lors C., Ponge J.-F., Caron L., Biaz A., Dazy M. and Masfaraud J.-F. (2012) Metal immobilization and soil amendment efficiency at a contaminated sediment landfill site: A field study focusing on plants, springtails, and bacteria. *Environmental Pollution* **169**, 1-11.

Bolan N.S., Park J.H., Robinson B., Naidu R., and Huh K.Y. (2011) Chapter four - Phytostabilization: A Green Approach to Contaminant Containment. *Advances in Agronomy*, **112**, 145-204.

Brown S., Chaney R., Hallfrisch J., Ryan J.A. and Berti W.R. (2004) In situ soil treatments to reduce the phyto- and bioavailability of lead, zinc, and cadmium. *Journal of Environmental Quality*, **33,** 522–531.

Bruno I., Cole J., Edgington P., Kessler M., Macrae C., McCabe P., Pearson J. and Taylor R. (2002) New software for searching the Cambridge Structural Database and visualising crystal structures. *Acta Crystallographica* B **58**, 389–397.

Carroll S. A., O'Day P. A., Esser B. and Randall, S. (2002) Speciation and fate of trace metals in estuarine sediments under reduced and oxidized conditions, Seaplane Lagoon, Alameda Naval Air Station (USA). *Geochemical Transactions* **3**, 81-101.

Cuny D., Denayer F.O., de Foucault B., Schumacker R., Colein P. and Van Haluwyn C. (2004) Patterns of metal soil contamination and changes in terrestrial cryptogamic communities. *Environmental Pollution*, **129**, 289-297.

de Livera J., McLaughlin M.J., Hettiarachchi G.M., Kirby J.K. and Beak, D.G. (2011) Cadmium solubility in paddy soils: Effects of soil oxidation, metal sulfides and competitive ions. *Science of the Total Environment*, **409** (8), 1489−1497.

Farinati S., DalCorso G., Panigati M. and Furini A. (2011) Interaction between selected bacterial strains and *Arabidopsis halleri* modulates shoot proteome and cadmium and zinc accumulation. *Journal of Experimental Botany*, **62**, 3433–3447.

Fulda B., Voegelin A., Ehlert K. and Kretzschmar R. (2013) Redox transformation, solid phase speciation and solution dynamics of copper during soil reduction and reoxidation as affected by sulfate availability. *Geochimica et Cosmochimica Acta* **123**, 385-402.

Gomez-Balderas C.D.C., Cochet N., Bert V., Tarnaud E. and Sarde C.-O. (2014) 16S rDNA analysis of bacterial communities associated with the hyper accumulator *Arabidopsis halleri* grown on a Zn and Cd polluted soil. *European Journal of Soil Biology* **60**, 16-23.

Hamon, R.E., McLaughlin, M.J., Naidu, R., Correll, R. (1998) Long-term changes in cadmium bioavailability in soil. *Environmental Science and Technology* **32**, 3699-3703.

Hinsinger P. (1998) How do plant roots acquire mineral nutriments? Chemical processes involved in the rhizosphere. *Advances in* Agronomy, **64**, 225-265.

Hinsinger P., Plassard C., Tang C. and Jaillard B. (2003) Origins of root-mediated pH changes in the rhizosphere and their responses to environmental constraints: A review. *Plant and Soil*, **248**, 43–59.

Hinsinger P., Plassard C. and Jaillard B. (2006) Rhizosphere: A new frontier for soil biogeochemistry. *Journal of Geochemical Exploration* **88**, 210-213.

Huguet S., Bert V., Laboudigue A., Barthès V., Isaure M.P., Llorens I., Schat H. and Sarret G. (2012) Cd speciation and localization in the hyperaccumulator *Arabidopsis halleri*. *Environmental and Experimental Botany*, **82**, 54-65.

Isaure M.P., Laboudigue A., Manceau A., Sarret G., Tiffreau C., Trocellier P., Lamble G., Hazemann J.L. and Chateigner D. (2002) Quantitative Zn speciation in a contaminated dredged sediment by μ-PIXE, μ-SXRF, EXAFS spectroscopy and principal component analysis. *Geochimica et Cosmochimica Acta*, **66**, 1549-1567.

Isaure M.P., Manceau A., Geoffroy N., Laboudigue A., Tamura N. and Marcus M.A. (2005) Zinc mobility and speciation in soil covered by contaminated dredged sediment using

micrometer-scale and bulk-averaging X-ray fluorescence, absorption and diffraction techniques. *Geochimica et Cosmochimica Acta*, **69**, 1173-1198.

Isaure M.P., Fayard B., Sarret G., Pairis S. and Bourguignon J. (2006) Localization and chemical forms of cadmium in *Arabidopsis thaliana*. *Spectrochimica Acta B*, **61**, 1242–1252.

Isaure M.P., Huguet S., Meyer, C.L., Castillo-Michel H., Testemale D., Vantelon D., Saumitou-Laprade P., Verbruggen N. and Sarret G. (2015) Evidence of various mechanisms of Cd sequestration in the hyperaccumulator *Arabidopsis halleri*, the non-accumulator *Arabidopsis lyrata*, and their progenies by combined synchrotron-based techniques. *Journal of Experimental Botany.* **66**, 3201-3214.

Karlsson T., Persson P. and Skyllberg U. (2005) Extended X-ray absorption fine structure spectroscopy evidence for the complexation of cadmium by reduced sulfur groups in natural organic matter. *Environmental Science and Technology*, **39**, 3048-3055.

Karlsson T. and Skyllberg U. (2007) Complexation of zinc in organic soils - EXAFS evidence for sulfur associations. *Environmental Science and Technology*, **41**, 119-124.

Li T., Liang C., Han X. and Yang X. (2013) Mobilization of cadmium by dissolved organic matter in the rhizosphere of hyperaccumulator *Sedum alfredii*. *Chemosphere* **91**, 970-976.

Lions J., Guérin V., Bataillard P., Van der Lee J. and Laboudigue A. (2010) Metal availability in a highly contaminated, dredged-sediment disposal site: Field measurements and geochemical modelling. *Environmental Pollution*, **158**, 2857-2864.

Liu C., Frenkel A.I., Vairavamurthy A. and Huang P.M. (2001) Sorption of cadmium on humic acid: Mechanistic and kinetic studies with atomic force microscopy and X-ray absorption fine structure spectroscopy. *Canadian Journal of Soil Science*, **81** (3) Special Iss. SI, 337-348.

Lors C., Tiffreau C. and Laboudigue A. (2004) Effects of bacterial activities on the release of heavy metals from contaminated dredged sediments. *Chemosphere*, **56**, 619-630.

Marschner H. (1995) *Mineral nutrition of higher plants, second edition* Academic Press, London.

McBride M.B., Barrett K.A. and Martinez C.E. (2006) Zinc and cadmium distribution and leaching in a metalliferous peat. *Water Air and Soil Pollution*, **171**, 67-80.

Meyer C.L., Kostecka A.A., Saumitou-Laprade P., Créach A., Castric V., Pauwels M. and Frérot H. (2010) Variability of zinc tolerance among and within populations of the pseudometallophyte species *Arabidopsis halleri* and possible role of directional selection. *New Phytologist* **185**, 130–142

Meyer C.L., Juraniec M., Huguet S., Chaves-Rodriguez E., Salis P., Isaure M.P., Goormaghtigh E. and Verbruggen N. (2015). Intraspecific variability of cadmium tolerance and accumulation, and cadmium-induced cell wall modifications in the metal hyperaccumulator *Arabidopsis halleri*. *Journal of Experimental Botany*, **66**, 3215-3227.

Mishra B., Boyanov M., Bunker B.A., Kelly S.D., Kemner K.M. and Fein J.B. (2010) High- and low-affinity binding sites for Cd on the bacterial cell walls of *Bacillus subtilis* and *Shewanella oneidensis*. *Geochimica et Cosmochimica Acta*, **74**, 4219−4233.

Nolan A.L., Zhang H. and McLaughlin M.J. (2005) Prediction of zinc, cadmium, lead, and copper availability to wheat in contaminated soils using chemical speciation, diffusive gradients in thin films, extraction, and isotopic dilution techniques. *Journal of Environmental Quality*, **34**, 496-507.

O'Day P., Carrol S.A. and Waychunas G.A. (1998) Rock-Water interactions controlling zinc, cadmium, and lead concentrations in surface waters and sediments, US tri-state mining district. 1. Molecular identification using X-ray absorption spectroscopy. *Environmental Science and Technology*, **32**, 943-955.

Panfili F., Manceau A., Sarret G., Spadini L., Kirpichtchikova T., Bert V., Laboudigue A., Marcus M., Ahamdach N. and Libert M. (2005) The effect of phytostabilization on Zn speciation in a dredged contaminated sediment using scanning electron microscopy, X-ray

fluorescence, EXAFS spectroscopy and principal components analysis. *Geochimica et Cosmochimica Acta*, **69**, 2265-2284.

Pauwels M., Frérot H., Bonnin I. and Saumitou-Laprade P. (2006) A broad-scale analysis of population differentiation for Zn tolerance in an emerging model species for tolerance study: *Arabidopsis halleri* (Brassicaceae). *Journal of Evolutionary Biology*, **19**, 1838-1850.

Piou S., Bataillard P., Laboudigue A., Férard J.F. and Masfaraud J.F. (2009) Changes in the geochemistry and ecotoxicity of a Zn and Cd contaminated dredged sediment over time after land disposal. *Environmental Research*, **109**, 712-720.

Proux O., Nassif V., Prat A., Ulrich O., Lahera E., Biquard X., Menthonnex J.J. and Hazemann, J.L. (2006). Feedback system of a liquid-nitrogen-cooled double-crystal monochromator: design and performances. *Journal of Synchrotron Radiation* **13**, 59–69.

Ravel B. (2009). ATHENA Users' Guide, version 1.5
http://cars9.uchicago.edu/~ravel/software/doc/Athena/html/athena.pdf

Ravel B. and Newville M. (2005). ATHENA and ARTEMIS: interactive graphical data analysis using IFEFFIT. *Journal of Synchrotron Radiation*, **12**, 537–541.

Roosens N., Willems G. and Saumitou-Laprade P. (2008) Using *Arabidopsis* to explore zinc tolerance and hyperaccumulation. *Trends in Plant Science* **13**, 208-215.

Sajidu S.M.I., Masamba W.R.L., Thole B. and Mwatseteza J.F. (2008) Groundwater fluoride levels in villages of Southern Malawi and removal studies using bauxite, *International Journal of Physical Sciences,* **3**, pp. 001–011.

Sarret G., Connan J., Kasrai M., Eybert-Bérard L., Bancroft G.M. (1999). Characterization of sulfur in asphaltenes by sulfur K- and L-edge XANES spectroscopy. *Journal of Synchrotron Radiation*, **6**, 670-672.

Sarret G., Balesdent J., Bouziri L., Garnier J.M., Marcus M.A., Geoffroy N., Panfili F. and Manceau A. (2004) Zn speciation in the organic horizon of a contaminated soil by micro X-

ray fluorescence, micro and powder EXAFS spectroscopy and isotopic dilution. *Environmental Science and Technology*, **38**, 2792-2801.

Sarret G., Willems G., Isaure MP., Marcus M.A., Fakra S., Frérot H., Pairis S., Geoffroy N., Manceau A. and Saumitou-Laprade P. (2009) Zn distribution and speciation in *Arabidopsis halleri* x *Arabidopsis lyrata* progenies presenting various Zn accumulation capacities. *New Phytologist,* **184**, 581–595.

Szymanski J.T. (1978) The crystal structure of cernýite, Cu2CdSnS4, a cadmium analogue of stannite. *The Canadian Mineralogist*, **16**, 147-151

Thiry M., Huet-Taillanter S. and Schmitt J.M. (2002) The industrial waste land of Mortagne-du-Nord (59) - I - Assesment, composition of the slags, hydrochemistry, hydrology and estimate of the outfluxes. *Bulletin De La Societe Geologique De France,* **173**, 369-381.

Tsednee M., Yang S.-C., Lee D.-C., Yeh K.-C. (2014) Root-secreted nicotianamine from Arabidopsis halleri facilitates zinc hypertolerance by regulating zinc bioavailability. *Plant Physiology*, **166**, 839-852.

Vansimaeys C., Alary C., Bataillard P., Zentar R. and Laboudigue A. (2009) Ripening of contaminated sediments: effect on organic matter-bound and iron oxides-bound metals. International Conference on the Biogeochemistry of Trace Element (ICOBTE), Chihuahua, Mexico.

Verbruggen N., Juraniec M., Baliardini C. and Meyer C.-L. (2013) Tolerance to cadmium in plants: the special case of hyperaccumulators. *Biometals* **26**, 633–638.

Wenzel W.W. and Jockwer F. (1999) Accumulation of heavy metals in plants grown on mineralised soils of the Austrian Alps. *Environmental Pollution*, **104**, 145–155.

Wenzel W.W., Bunkowski M., Puschenreiter M. And Horak O. (2003) Rhizosphere characteristics of indigenously growing nickel hyperaccumulator and excluder plants on serpentine soil. *Environmental Pollution*, **123**, 131-138.

Wenzel W.W. (2009) Rhizosphere processes and management in plant-assisted bioremediation (phytoremediation) of soils. *Plant and Soil*, **321**, 385-408.

Zhang H., Zhao F.J., Sun B., Davison W. and McGrath S.P. (2001) A new method to measure effective soil solution concentration predicts copper availability to plants. *Environmental Science and Technology*, **35**, 2602-2607.

Table captions

Table 1: General properties of studied sediment. Averages and standard deviations over 3 samples.

Table 2: First shell structural parameters by shell fittings of the EXAFS spectra for sediment samples before and after culture, with or without plant, and for references.

Figure captions

Figure 1: Schema summarizing the design of culture experiment. *ti* means « initial time » that corresponds to the time of *A. halleri* seedlings transfer in sediment. The monitoring was done every month from the time t_0.

Figure 2: Cd K-edge EXAFS spectra for reference compounds including $CdCO_3$ (powder); $Cd(OH)_2$ (powder); $CdCl_2$ (powder); $CdSO_4$ (powder); Cd-goethite : 0.8% Cd (powder); Cd-phosphate : $Cd_5H_2(PO_4)_4.4H_2O$ (powder); $Cd(NO_3)_2$ (powder); Cd^{2+} : 10 mM Cd^{2+} at pH=2.2 (Cd dissolved form); Cd-cellulose : described in Isaure et al., 2006; Cd-OAs : 5 mM Cd, 14 mM citrate, 100 mM malate and 400 mM succinate at pH 5.5; Cd-cysteine : (Zn, Cd, Fe)S as mixed sulfide (powder) characterized by XRD; CdS (powder).

Figure 3: (A) Cd K-edge EXAFS spectra for sediment before and after culture, with or without plant. Each spectrum (plain lines) is shown with its linear combination fit (dotted lines). (B) Distribution of Cd species for samples after normalization of the percentage to 100%.

Figure 4: Cd K-edge EXAFS spectra (A) and Fourier transforms (B) for sediment before and after culture, with or without plant, and for references: $CdCO_3$ and Cd-phosphate as representative of Cd-O bonds and CdS and (Zn, Cd, Fe)S as representative of Cd-S ligands. Each spectrum (plain lines) is shown with their shell fittings (dotted lines).

Figure 5: SEM EDS images and EDS spectrum recorded in Cd-rich spot of a coarse fraction grain of sediment before culture (A) and elemental maps for Cd, S and P of this region

recorded by μXRF (B), with a step-size of 3μm and 1s/pixel of counting time. Spots were called "P1-before culture" and "P2-before culture".

Figure 6: Light microscope and SEM EDS images of a coarse grain of sediment after culture with MET plant and EDS spectrum recorded in Cd-rich spot (A), and elemental maps for Cd, S, P, Si and Al of this region recorded by μXRF (B), with a step-size of 3μm and 1s/pixel of counting time. Spots were called "P3A-after culture", "P3B-after culture" and "P3C-after culture". Another Cd-rich grain was investigated: elemental maps for Cd, S, P, Si and Al of this other region recorded by μXRF (C), with a step-size of 3μm and 1s/pixel of counting time. Spot was called "P4-after culture".

Figure 7: Cd L_{III}-edge XANES spectra of bulk sediment before culture and reference compounds (XANES spectra) and μXANES spectra recorded on Cd-rich spots of sediment before culture and after culture with MET plant. Experimental spectra are in plain lines and best linear combination fits are in dotted lines. Reference compounds representative of Cd-O ligands are $CdCO_3$, Cd-organic acid (Cd-malate), and representative references of Cd-S ligands are Cd-thiol (Cd-cysteine), and sulfides: CdS and (Zn, Cd, Fe)S.

Figure 8: S K-edge XANES spectra of bulk sediment before culture and reference compounds (XANES spectra) and μXANES spectra recorded on Cd-rich spots of sediment before culture and after culture with MET plant. Experimental spectra are in plain lines and best linear combination fits are in dotted lines. Reference compounds are oxided sulfur (Cd-sulfate), sulfoxide (DL-methionine sulfoxide, from Sarret et al., 1999), organic sulfide (DL-cysteine, from Sarret et al., 1999) and mineral sulfides (CdS and (Zn, Cd, Fe)S).

Figure 9: Distribution of Cd (A) and S (B) species for samples after normalization of the percentage to 100%. Percentages presented are the average over satisfactory fits, defined by NSS comprised between the value obtained for the best fit (NSS_{best}) and 1.1 NSS_{best}.

Figure 10: Comparison between concentrations of Cd extractable measured by $Ca(NO_3)_2$ extraction (A) and Cd phytoavailability estimated by DGT (B), in the sediment cultivated with MET and N-MET plants (grey and white respectively), and in the control (without plant - hatched). All data are averages ± SD over 3 samples. "PA" means "plant adaptation". On each graph, results of statistical tests are indicated by Latin and Greek letters for MET plant

culture and N-Met plant culture respectively. A different letter indicates a significant difference at the *P*=0.05 level.

Figure 11: (A) Cd concentrations [mg.L-1] measured in leachates collected from cultivated pots with MET plant (grey) and N-MET plant (white) origins and non cultivated pot as a control (hatched), (B) biomass and (C) Cd concentrations measured in aerial parts of *A. halleri* from MET and N-MET origins. Averages and standard deviations are over 3 samples. For each graph, results of statistical tests are indicated by Greek and Latin letters for pots with MET plant and N-MET plant respectively. A different number or letter indicates a significant difference at the *P*=0.05 level. There is no significant difference of Cd concentration in leachates measured in control pots without plant.

Table 1

Clay < 2 μm	%	18 ± 0.5	(3)
Silt 2μm - 50 μm	%	45 ± 1	(3)
Sand 50μm - 2 mm	%	36 ± 1	(3)
CaCO$_3$ (total)	%	7.2 ± 0.2	(3)
TOC	%	10.5 ± 0.2	(3)
pH, H$_2$O		7.48 ± 0.01	(3)
OM	g kg^{-1}	225 ± 1.3	(3)
CEC Metson	cmol(+) kg^{-1}	25.4 ± 0.5	(3)
K (K$_2$O) exchangeable	g kg^{-1}	0.24 ± 0.02	(3)
Mg (MgO) exchangeable	g kg^{-1}	0.599 ± 0.003	(3)
Ca (CaO) exchangeable	g kg^{-1}	15.47 ± 0.06	(3)
Na (Na$_2$O) exchangeable	g kg^{-1}	0.205 ± 0.003	(3)
P (P$_2$O$_5$) Olsen	g kg^{-1}	0.227 ± 0.003	(3)
Cd concentration	mg kg^{-1}	141 ± 24	(3)
Zn concentration	mg kg^{-1}	4074 ± 280	(3)
Cu concentration	mg kg^{-1}	233 ± 9	(3)
Pb concentration	mg kg^{-1}	600 ± 20	(3)
Ni concentration	mg kg^{-1}	48 ± 2	(3)
As concentration	mg kg^{-1}	57 ± 4	(3)

Table 2

References and Samples	K range (Å^{-1})	R range (Å)	Atom	N	R (Å)	σ^2 (Å^2)	NSS
CdCO$_3$	[3.2 - 14.7]	[1.35 - 4.1]	O	6.2	2.28	0.004	
			C	6.1	3.18	0.005	0.0090
			O	5.8	3.40	0.005	
			Cd	6,0	3.93	0.004	
Cd-phosphate	[3.2 - 14.3]	[0.88 - 4.5]	O	6.1	2.27	0.008	
			P	2.9	3.44	0.009	0.0110
			Cd	1.7	3.50	0.009	
CdS	[3.5 - 13.9]	[1.37 - 4.7]	S	4,0	2.52	0.003	0.0150
			Cd	10.4	4.14	0.007	
(Zn. Cd. Fe)S mixed sulfide	[3.6 - 13.4]	[1.32 - 4.6]	S	4,0	2.52	0.004	
			Fe	0.4	3.69	0.009	0.0190
			Zn	5,0	3.89	0.009	
			Cd	2.5	4.18	0.009	
Sediment - before culture Adjustment with (Zn, Cd, Fe)S structure	[3.6 - 13.4]	[1.35 - 4.3]	S	4,0	2.51	0.004	
			Fe	0.3	3.69	0.009	0.0024
			Zn	4.8	3.89	0.009	
			Cd	2.2	4.17	0.009	
Sediment - before culture Adjustment with (Zn, Cd, Fe)S Structure without Fe atoms	[3.6 - 13.4]	[1.35 - 4.3]	S	4.2	2.51	0.004	
			Zn	4.3	3.89	0.009	0.0037
			Cd	3.1	4.17	0.009	
Sediment without plant after culture	[3.2 - 10.8]	[1.2 - 2.9]	O	5.5	2.29	0.010	0.0026
			S	0.6	2.47	0.010	
Sediment with MET plant after culture	[3.2 - 10.8]	[1.2- 2.3]	O	6.7	2.29	0.009	0.0039
Sediment with N-MET plant after culture	[3.2 - 10.8]	[1.2 - 2.3]	O	6.2	2.30	0.009	0.0057

N: number of atoms, R: interatomic distance, σ2: Debye Waller factor, NSS: residual between fit and experiment. Experimental errors on N and R are ± 10% and 0.01 Å as estimated from the fit of reference compounds.

Figure 1.

Figure 2.

A

k³ ϰ(k)

k (Å⁻¹)

Sed-before culture

Sed-after culture without plant

Sed-after culture with MET plant

Sed-after culture with N-MET plant

B

Cd-Mineral sulfide

Cd-Phosphate

Cd-Organic acids

Percentage of Cd species

Figure 3.

A

(Zn, Cd, Fe)S

CdS

Sed-before culture
fit with S and Cd

Sed-before culture
fit with S, Zn, Cd and Fe

Sed-after culture
without plant

Sed-after culture
with MET plant

Sed-after culture
with N-MET plant

Cd-phosphate (powder)

CdCO$_3$

$k^3 \chi(k)$

k (Å^{-1})

B

FT magnitude

R + ΔR (Å)

Figure 4.

P1-before culture

P2-before culture
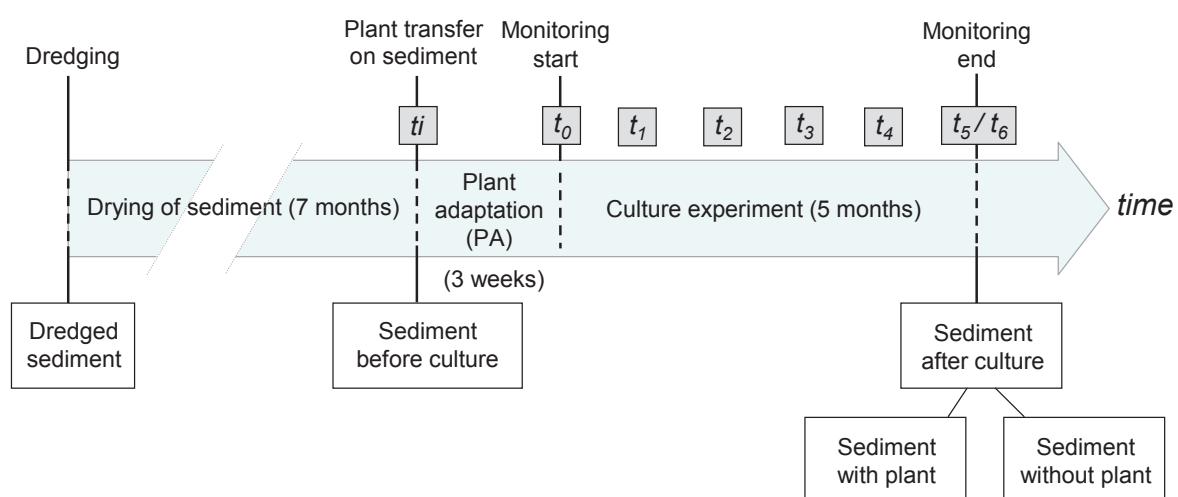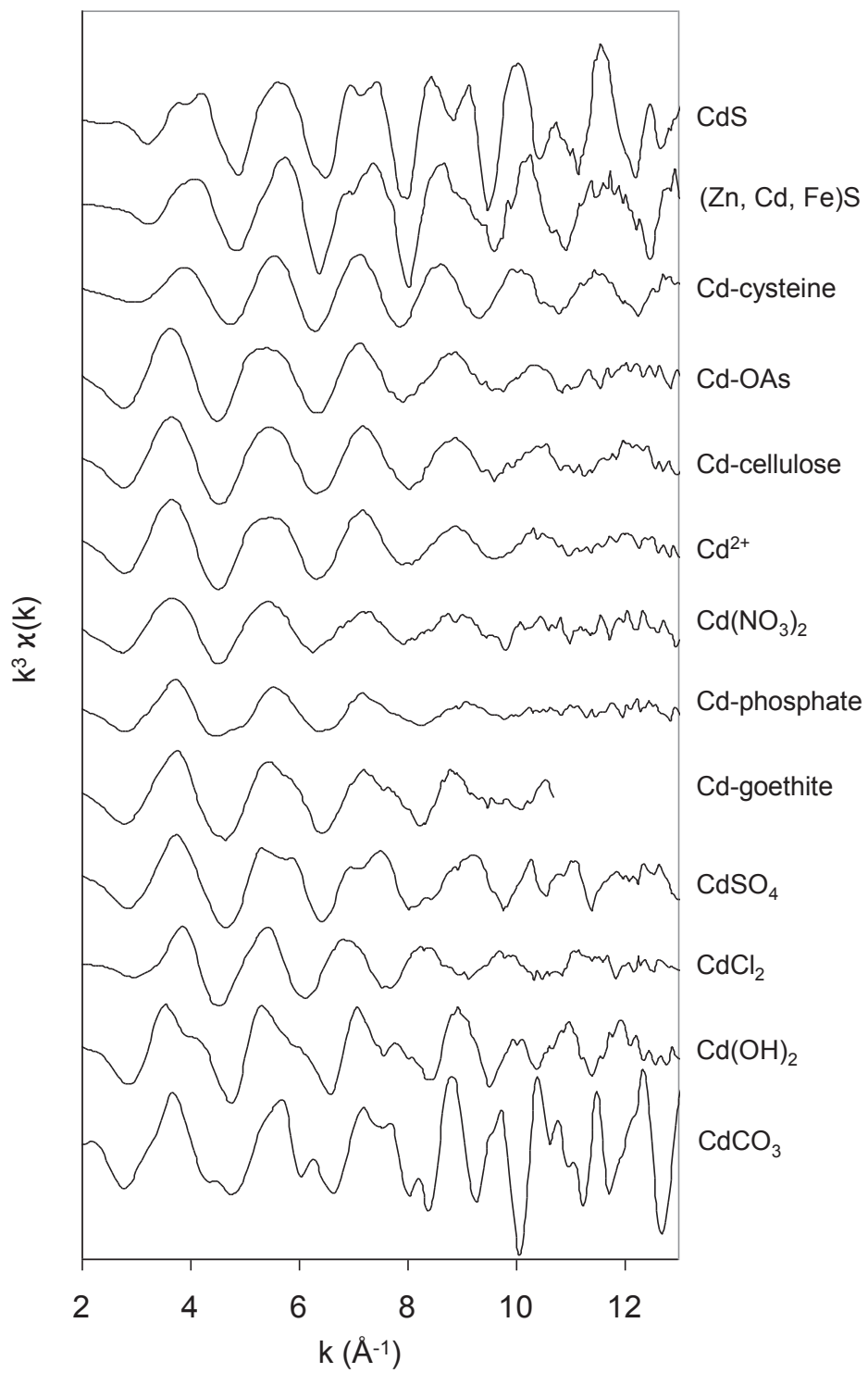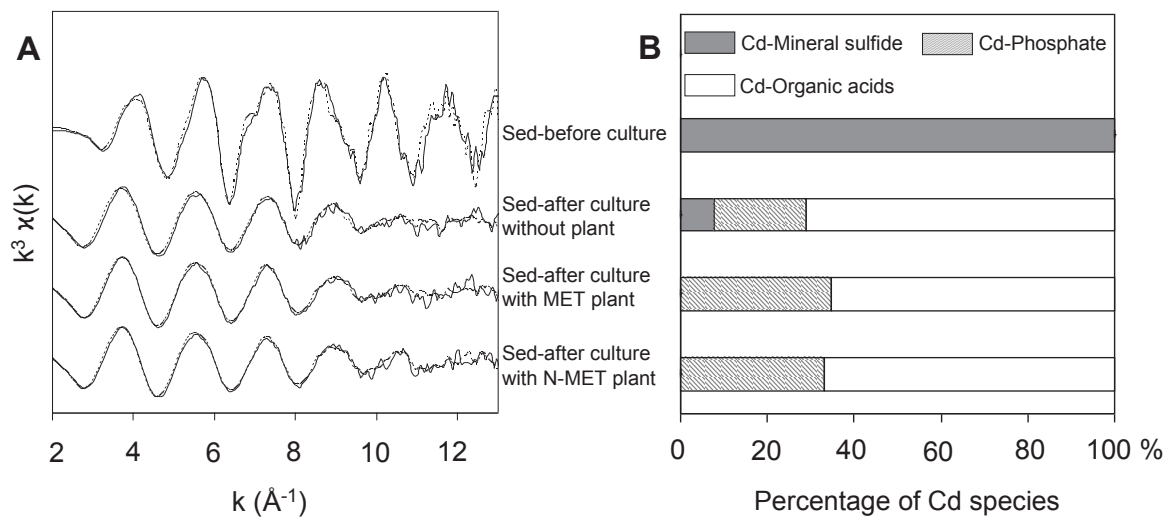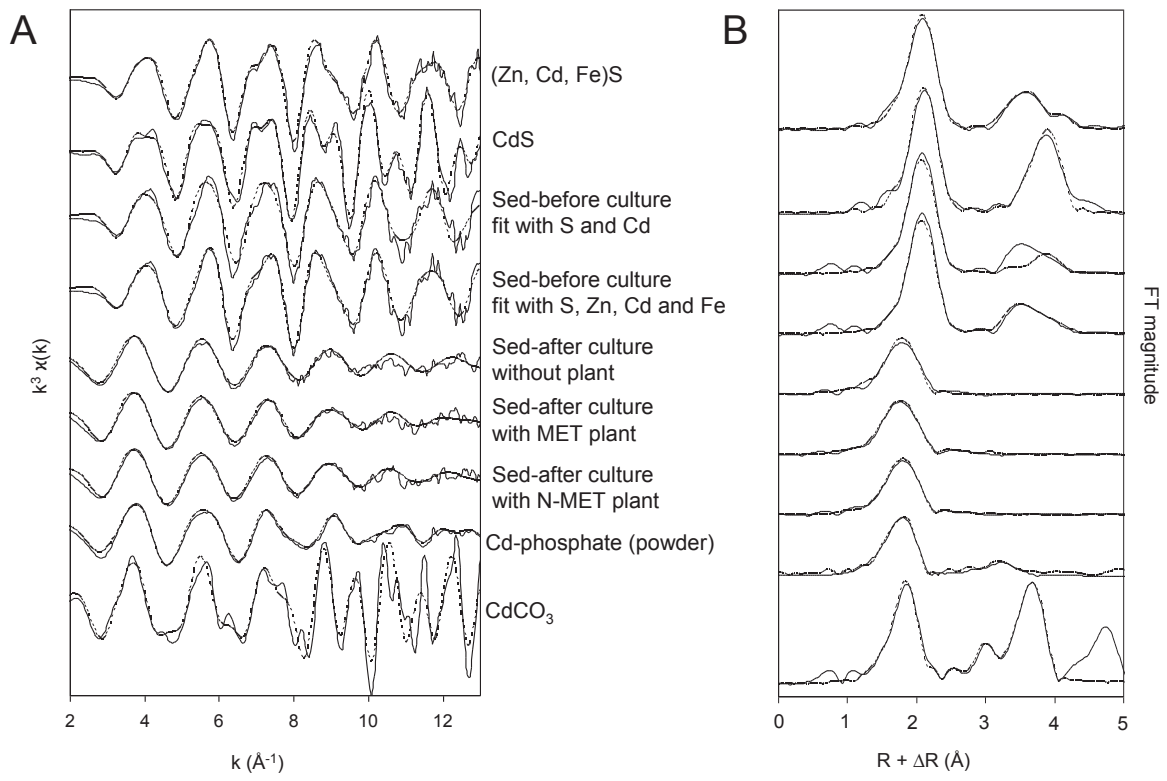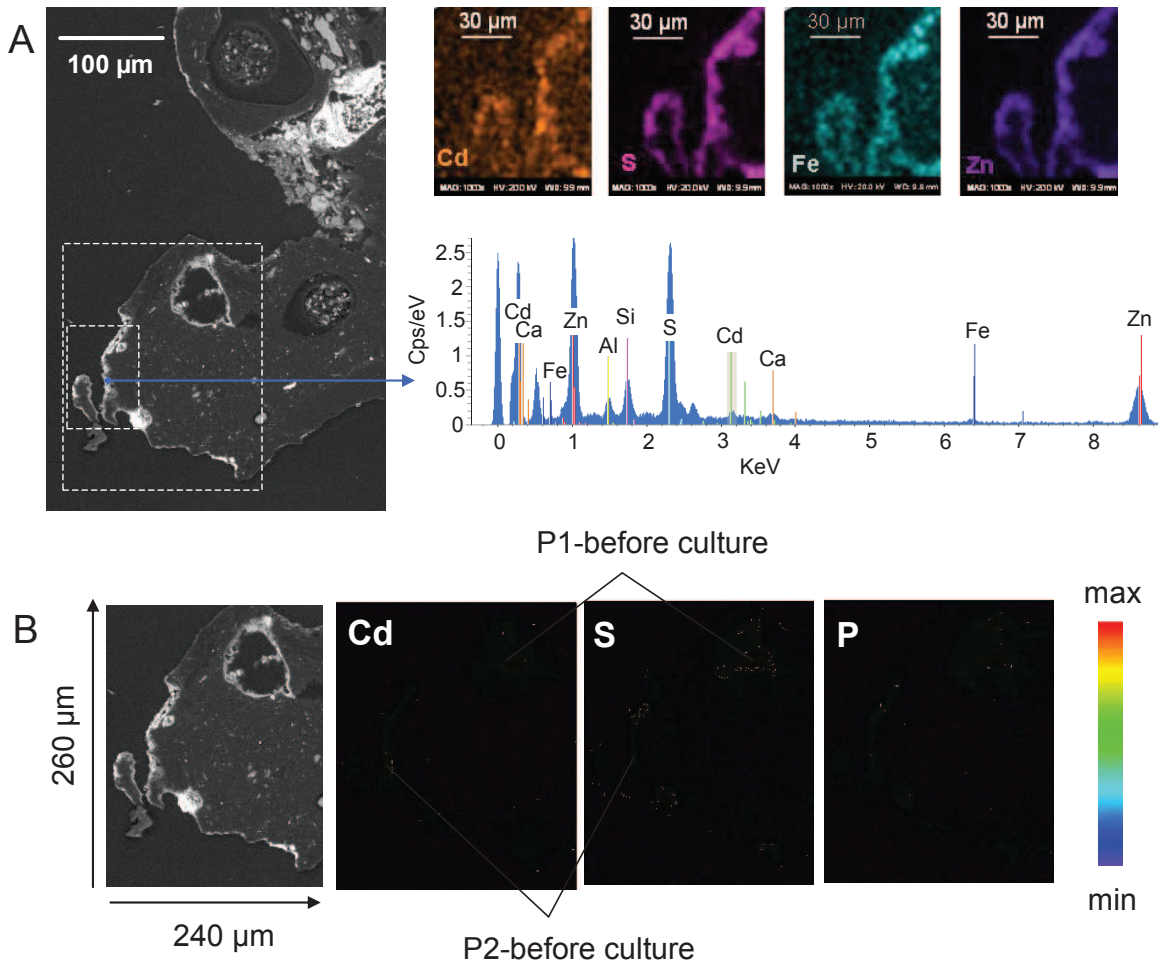
Figure 5.

Figure 6.

Figure 7.

Normalized absorbance

Sulfate : CdSO$_4$

O
‖
Sulfoxide : C-S-C

Organic sulfide :
DL-cysteine

Sulfide : CdS

Sulfide :(Zn,Cd,Fe)S

P4-after culture

P3C-after culture

P3B-after culture

P3A-after culture

P2-before culture

P1-before culture

Sediment bulk
before culture

Energy (eV)
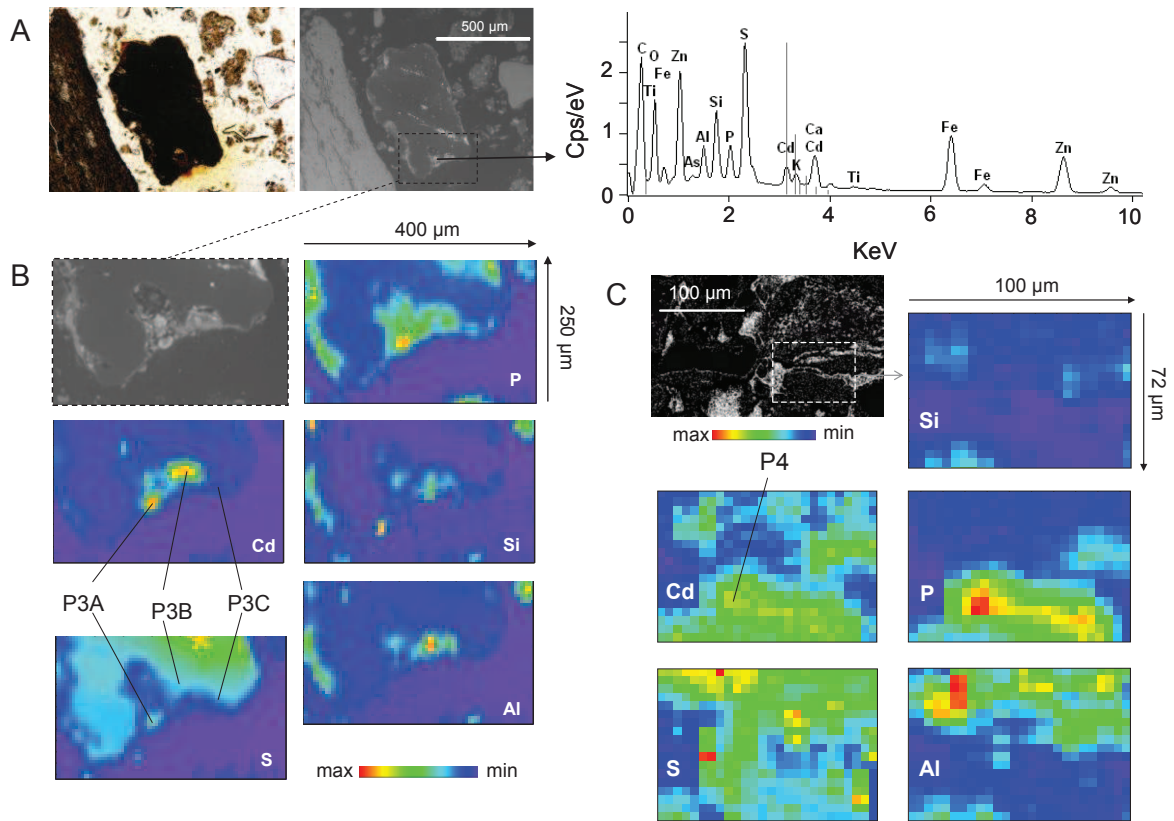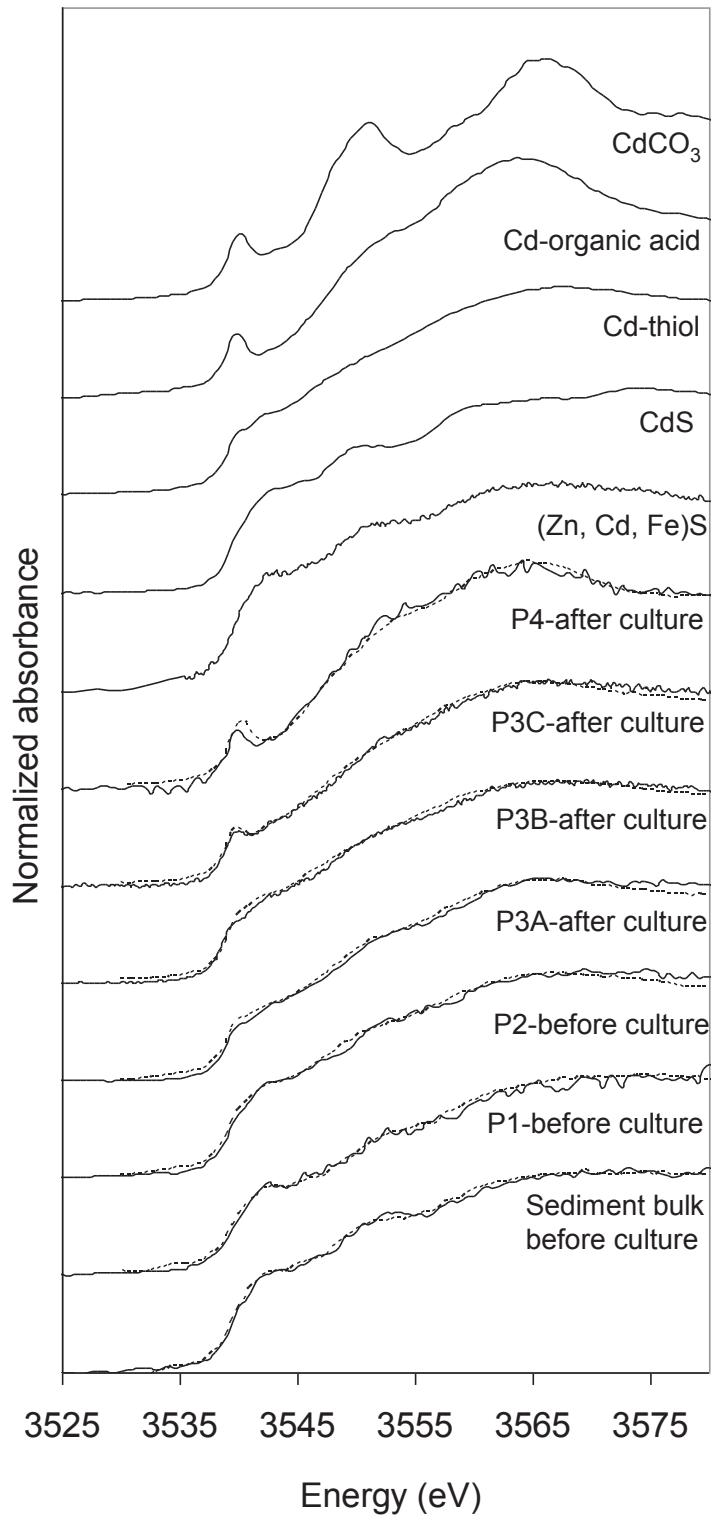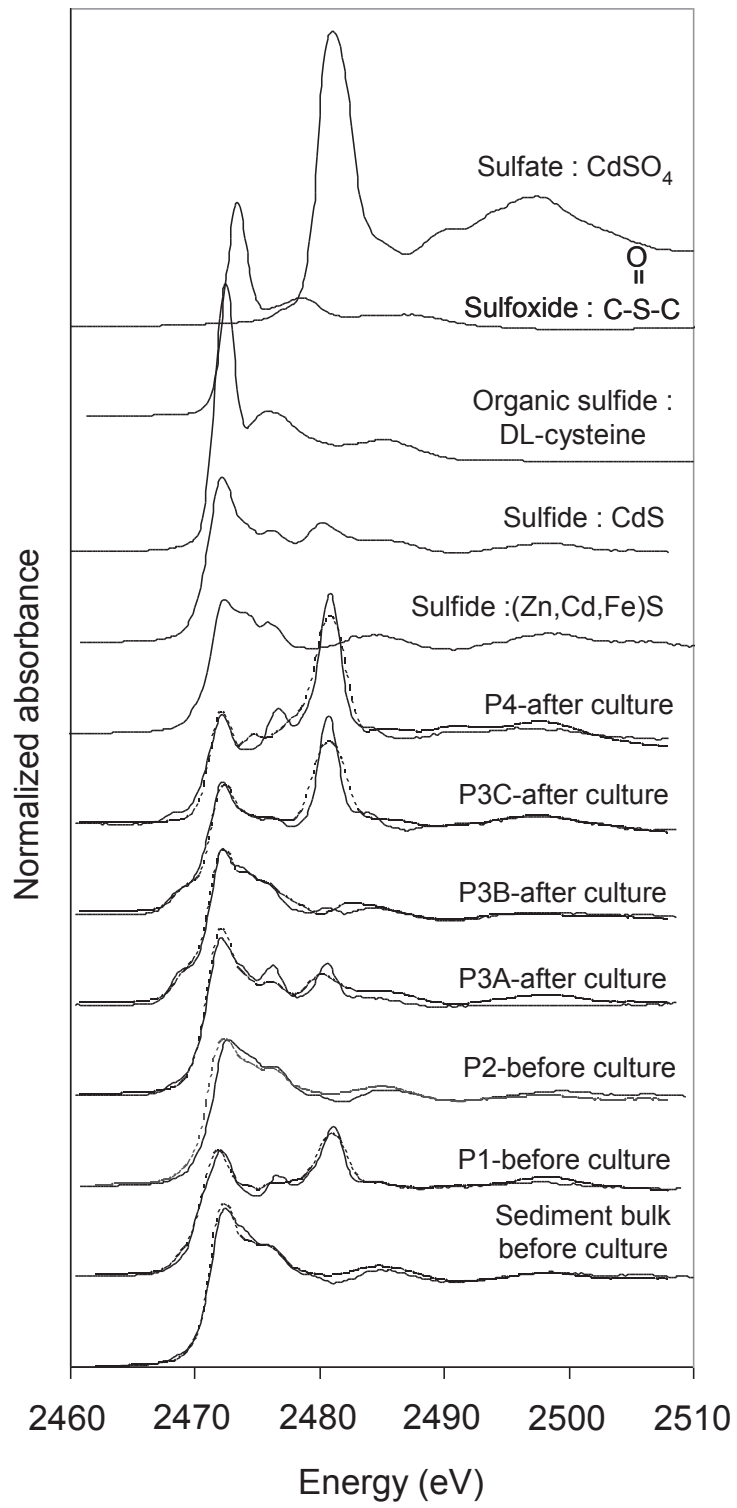
Figure 8.

A   Cd species (Cd L$_{III}$-edge)   **B**   S species (S K-edge)

Cd-Mineral sulfide   Cd-phosphate   Mineral sulfide   Organic sulfide
Cd-Organic sulfide   Cd-Organic acid   Oxidized sulfur

Sediment bulk before culture
P1-before culture
P2-before culture
P3A-after culture
P3B-after culture
P3C-after culture
P4-after culture

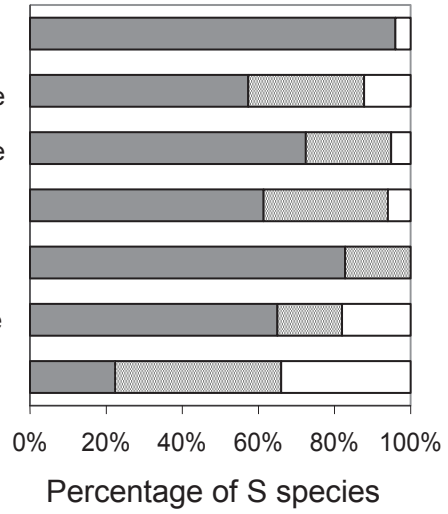Percentage of Cd species

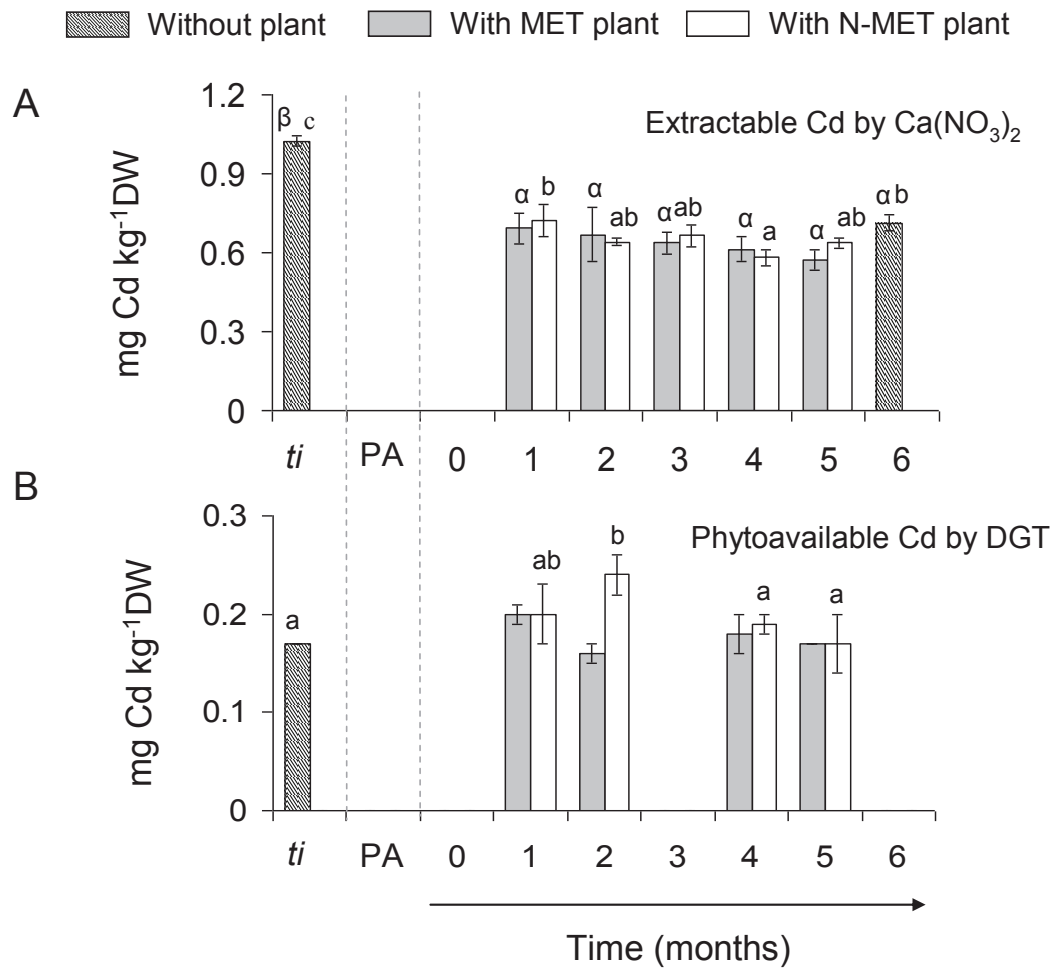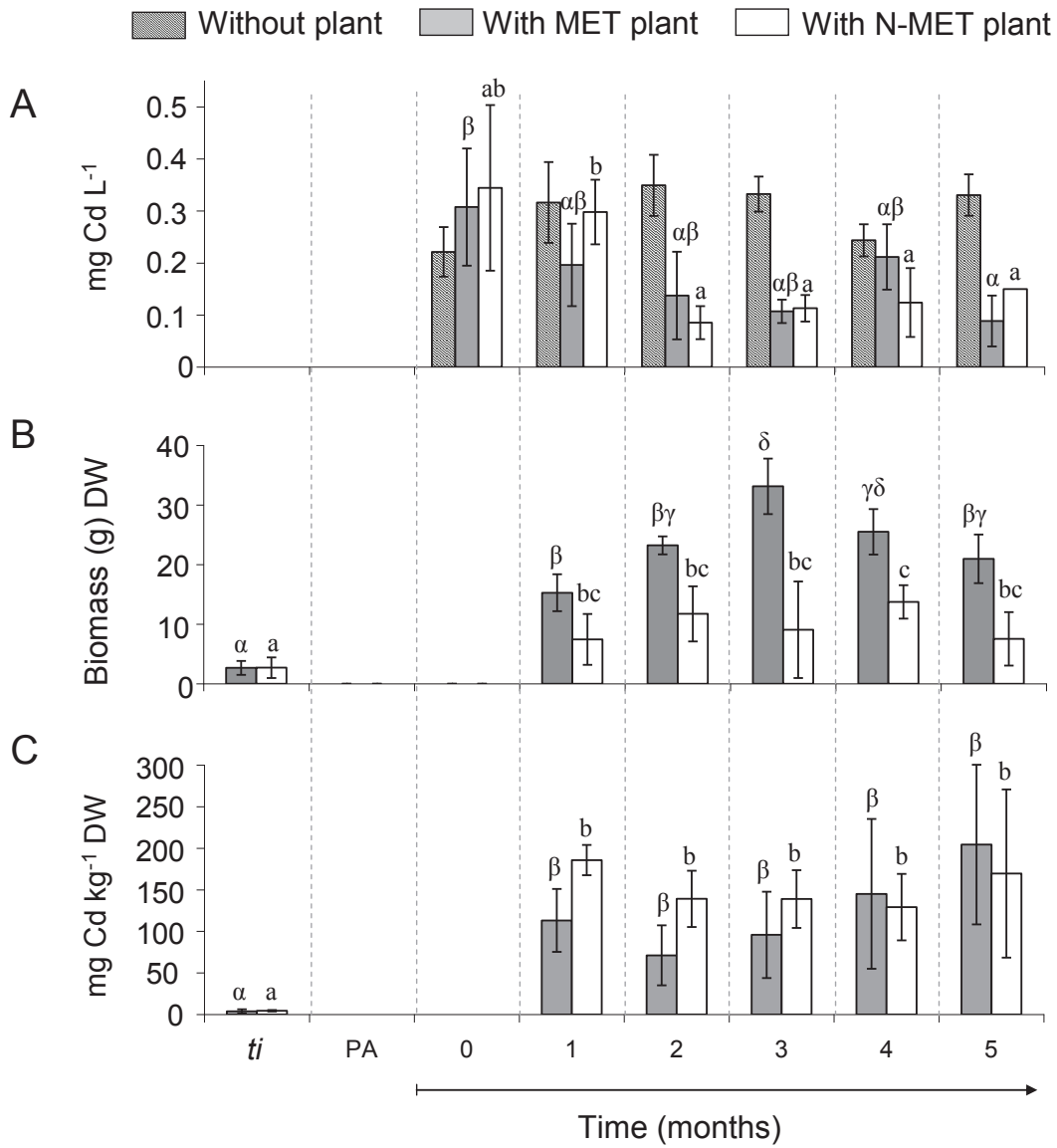Percentage of S species

Figure 9.

Figure 10.

Figure 11.

Supplementary material for on-line publication only
Click here to download Supplementary material for on-line publication only: SI_S-Huguet_STotEn.pdf

Supporting informations_Science of Total Environment

Article : "Fate of cadmium in the rhizosphere of *Arabidopsis halleri* grown in a contaminated dredged sediment".

Huguet Stéphanie, Isaure Marie-Pierre, Bert Valérie, Laboudigue Agnès, Proux Olivier, Flank Anne-Marie, Vantelon Delphine and Sarret Géraldine

		Hautes Fagnes soil		Auby soil (Sarret et al., 2004)
Clay < 2 µm	%	19	(1)	$\begin{bmatrix} 54 \end{bmatrix}$*
Silt 2µm - 50 µm	%	64	(1)	
Sand 50µm - 2 mm	%	17	(1)	46
$CaCO_3$ (total)	%	0.3	(1)	
TOC	%	9.16 ± 0.9	(3)	
pH, H_2O		6.94 ± 0.05	(3)	6.2
OM	g kg^{-1}	278	(1)	403
CEC Metson	cmol(+) kg^{-1}	29.5	(1)	52.7 ± 1.6*
K (K_2O) exchangeable	g kg^{-1}	0.18	(1)	0.985 ± 0.004*
Mg (MgO) exchangeable	g kg^{-1}	0.15	(1)	1.123 ± 0.011*
Ca (CaO) exchangeable	g kg^{-1}	3.23	(1)	13.06 ± 0.03*
Na (Na_2O) exchangeable	g kg^{-1}	1.86	(1)	0.0352 ± 0.0003*
P (P_2O_5) Olsen	g kg^{-1}	0.04	(1)	2.0
Cd concentration	mg kg^{-1}	0.90 ± 0.21	(15)	270
Zn concentration	mg kg^{-1}	88 ± 20	(15)	21078
Cu concentration	mg kg^{-1}	24.8 ± 4.3	(15)	406
Pb concentration	mg kg^{-1}	109 ± 15	(15)	9135
Ni concentration	mg kg^{-1}	18.5 ± 2.9	(15)	
As concentration	mg kg^{-1}	17.7 ± 2.8	(15)	

* Value including clays and silts

Figure SI-1: General properties of two different soils where *A. halleri* seeds were collected : Grain size distribution, sediment carbonate content ($CaCO_3$), Organic total carbonate (TOC), pH, organic matter content (OM), cation exchange capacity (CEC), exchangeable cations and heavy metal concentrations. Averages and standard deviations over (n) samples.
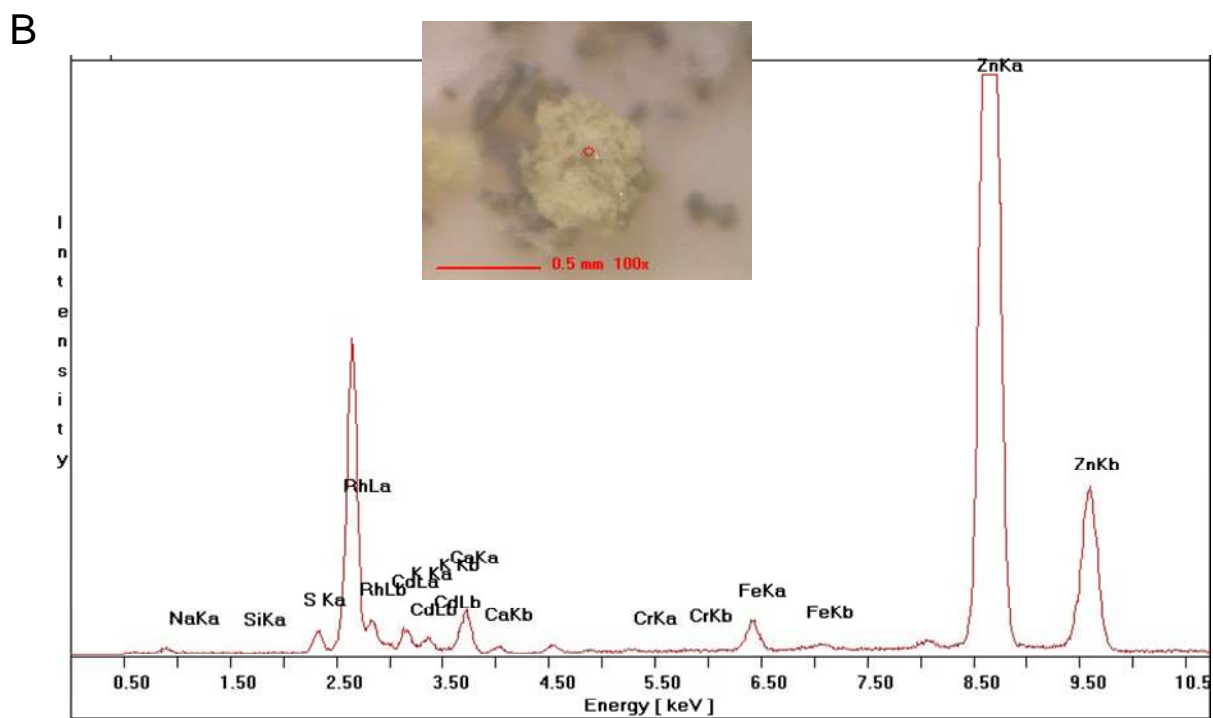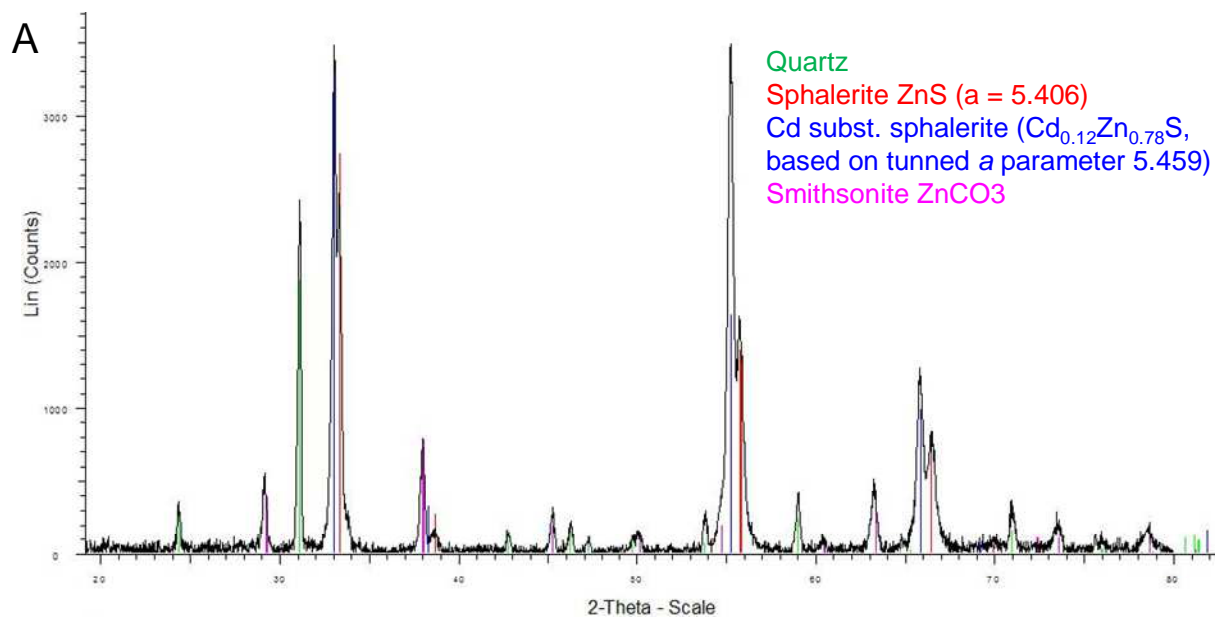
Figure SI-2: Characterization of the natural mixed sulfide reference: A: X-ray diffractogram. B: µXRF spectrum (incident beam: 40 kV, 200 µA)
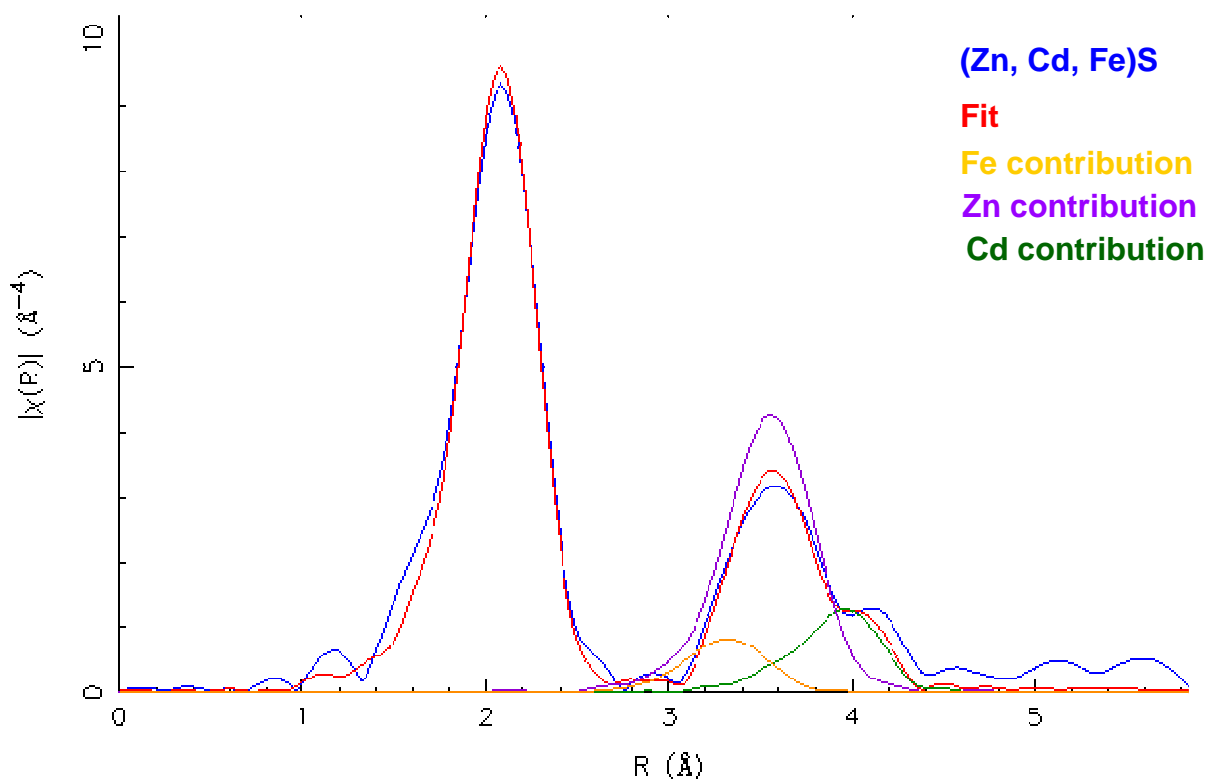
Figure SI-3: Fourier transform modulus of the k^3.chi(k) spectrum for the mixed sulfide (Zn, Cd, Fe)S reference compound (blue) and shell fitting (red). Fe, Zn and Cd individual contributions for the second shell are shown.